Nanoparticle Agglomeration via Ionic Colloidal Destabilization as a Novel Approach to Dry Powder Formulations for Pulmonary Drug Delivery

By

Carl J. Plumley
B.S. Vanderbilt University
Nashville, TN

Submitted to the graduate degree program in
Chemical and Petroleum Engineering and the Faculty of the
Graduate School of the University of Kansas in partial fulfillment of the
Requirements for the degree of Master's of Science

_____

Prof. Cory Berkland (Chair)

Committee Members**:** _____

Prof. Stevin Gehrke

_____

Prof. Javier Guzman

Date Defended: _____

Nanoparticle Agglomeration via Ionic Colloidal Destabilization as a Novel Approach to Dry Powder Formulation for Pulmonary Drug Delivery

By

Carl J. Plumley
B.S. Vanderbilt University
Nashville, TN

Submitted to the graduate degree program in
Chemical and Petroleum Engineering and the Faculty of the
Graduate School of the University of Kansas in partial fulfillment of the
Requirements for the degree of Master's of Science

_____

Prof. Cory Berkland (Chair)

Committee Members**:** _____

Prof. Stevin Gehrke

_____

Prof. Javier Guzman

Date Approved: _____

Abstract

Efficient administration of poorly water soluble drugs represents a leading challenge in pulmonary medicine. This route of administration has been used for steroidal treatments for some time, but with room for advancement. New inhalable medicines require a more reliable and effective dosing regimen due to narrow therapeutic indices, and specific and enhanced deposition in the lungs is also desired. This thesis investigates a general method for producing micron sized dry powders for a general class of drugs, poorly water soluble small molecule drugs, for their use in pulmonary drug delivery. Formulation methods already exist for inhalable aerosols, but the resulting powders often show limited deposition efficiency in the deep lung. In this body of work, an alternative formulation strategy is provided for inhalable dry powders using nanoparticle agglomeration that results in a potentially more efficient line of therapy. The model drug used in this study was nifedipine, a well known calcium channel blocker used to treat various symptoms of hypertension. The results indicated that nanoparticle agglomeration is a viable means of creating dry powders with suitable characteristics for pulmonary drug delivery as an alternative to more expensive and less controllable formulation strategies.

Dedicated to my family,

For their endless outpouring of strength and inspiration.

Acknowledgements

I would like to greatly thank my advisor, Dr. Cory Berkland, for his indispensable knowledge and guidance throughout my research. His encouragement for growth and perseverance is a dependable force amidst the trials of life and learning. I want to extend my utmost gratitude to all my peers and coworkers. Their support and help have allowed me to become a functional scholar and professional. Also, I would like to thank Dr. Stevin Gehrke and Dr. Javier Guzman for serving on my thesis committee and for all their attention and consideration in bringing me towards these achievements. °

I would like to thank Professor Eric Munson and his graduate student, Eric Gorman, for training and access to the DSC machinery in their laboratory. I would also like to thank Dr. John Haslam for his assistance and permission in using the Aerosizer apparatus in his laboratory. Additionally, I would like to thank Dr. David Moore and Heather Shinogle for all of their assistance and permission in using the SEM equipment in the KU Microscopy and Analytical Imaging Laboratory.

Finally, I would like to acknowledge funding from the Cystic Fibrosis Foundation.

Table of Contents

Appendix

A. Preliminary Studies

B. Cascade Impactor

Resources

Chapter One: Particulates for Pulmonary Drug Delivery

Drug delivery is a rapidly growing field of research, and pulmonary drug delivery has seen numerous advances in recent years.[1] As technologies become more adept at characterizing and manipulating microscopic and submicron materials, the ability to reliably produce entities on this scale continually improves. Drug delivery science has rapidly sought to put these improvements to application.[2] Traditionally, nanoparticles and microparticles have represented the primary delivery vehicles for a host of drugs, where 'nanoparticles' denotes pieces of material with diameters between 1 and 1000 nm and 'microparticles' have diameters between 1 and 1000 μm. The "ideal" drug nanoparticle may be equipped with a milieu of functions; everything it needs to carry out any number of activities on the cellular level.[3] A perfect nanoscale drug carrier may be many years away, but rudimentary nano- and microparticles still yield enormous benefits compared to traditional dosage forms.[4] In the past few decades, it has become clear that particulates are a benchmark design strategy for drug delivery scientists, representing a fundamental challenge for those interested in pulmonary delivery.[5]

Two general classes of particulates may be studied in pulmonary delivery: nanoparticles and microparticles. Microparticles are an effective vehicle for pulmonary drug delivery.[6] If they are manufactured in the correct size range, anywhere between 1 and 5 μm, they can reliably deposit into the terminal bronchioles and alveolar regions of the pulmonary bed.[7] Also, if their densities are

sufficiently low, anything less than ~0.4 g/cm^3, then particles greater than 5 μm may be used.[6] This prepared study focused on the storage and aerosolization of microparticle dry powders and determine their performance in the pulmonary airways. These powders are delivered to the lungs via dry powder inhalers (DPIs), as opposed to nebulized liquid droplets or pressurized suspensions of drugs that are stored in metered dose inhalers (MDIs).[8-10] DPIs characteristically rely on the force provided by a patient's inhalation to disperse and transport the particles into the lungs.[9] The following figure represents the steps involved in delivering powders to the lungs with a DPI.

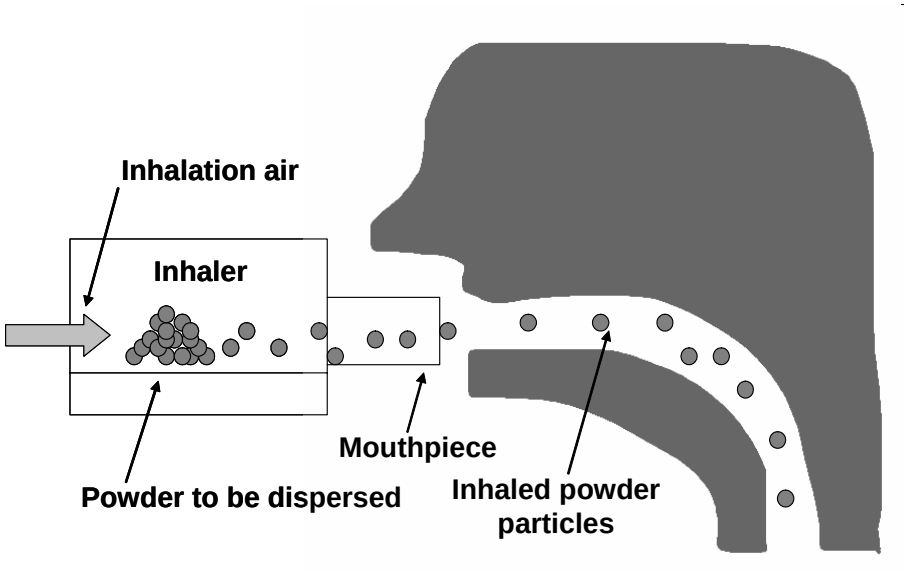

Figure 1.1 Diagram of a generalized dry powder inhaler in action. Adapted from Finlay, 2001.

The method of aerosolization is in contrast to MDIs, which almost always contain some sort of propellant which pressurizes the contents of their drug containing vessel, and this pressure provides the force necessary to push the nebulized liquid droplets into the patient's airways.[9] The DPI's mode of dispersal can cause insufficient aerosolization, especially if a patient exhibits weak inspiration as is often the case with diseased lung tissue.[11] DPIs require no coordination with a forced dose, include no environmentally harmful propellants, and are often cheaper to manufacture.

Dry particles may deposit along the airways via three primary mechanisms: Inertial impaction, sedimentation, and diffusion.[9,12-15] These events, though mostly noncompetitive, may all occur for a single dose of particles. They are represented in the figure below.

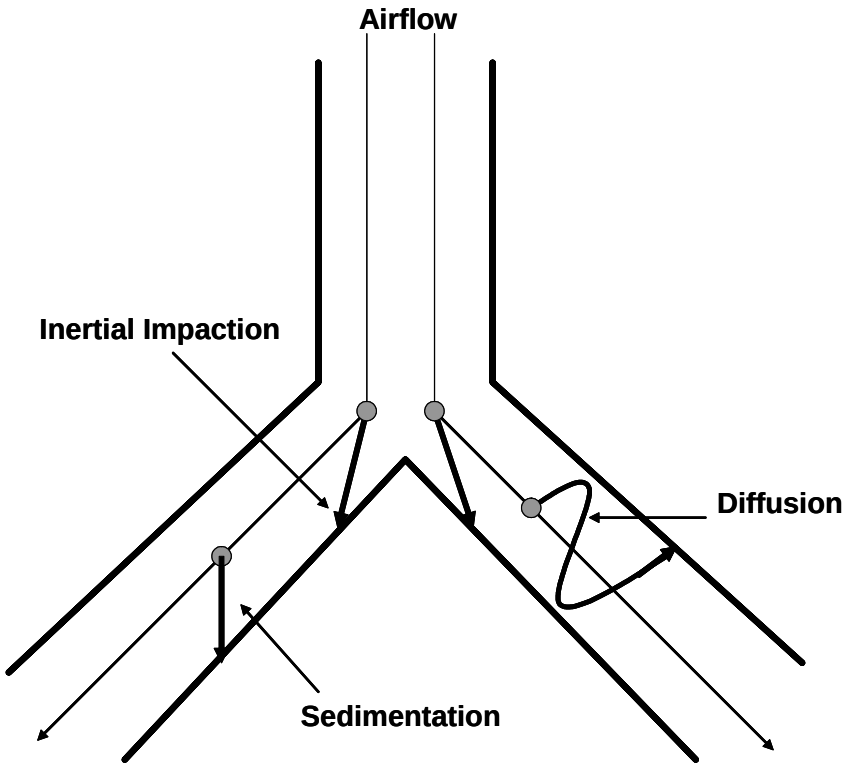

Figure 1.2 Diagram of the three non competing drug transport events that occur during pulmonary drug delivery. Adapted from Hillary, *et al.,* 2001.

Sedimentation refers to the gravitationally guided deposition of particles along the pulmonary airways. In most models, particles enter the airways with a velocity field that is parallel to the axial direction, and subsequently fall vertically upon the walls of the cylinder.[13] This mechanism dominates in the lower airways, and so may be exploited in deep lung delivery.[9] Enhanced deposition by this method is heavily dependent on time and this is one reason patients are asked to hold their breath upon inhalation.[9,14,15]

Inertial impaction refers to the deposition of particles as they stray from the angled air flow lines that pass through the many lung bifurcations. The particles

are unable to follow the velocity field because of their inherent inertia and their momentum straight forward is greater than the pull of the airflow around the curved bronchial tubes. This is commonly found to be the primary means of deposition for particles greater than 1 μm.[9] Porous particles, however, have recently been investigated for their ability to avoid premature deposition due to impaction.[15] Aerodynamic diameter is a very influential parameter for controlling inertial impaction. A geometrically large particle with a small aerodynamic diameter essentially means that the particle moves as if it were a much smaller particle of unit density. A smaller particle carries with it a smaller amount of inertia and so this translates to a lower susceptibility to inertial impaction. The governing equation is shown below.

$$d_{ae} = \left(\frac{\rho_{particle}}{\rho_{water} \times \lambda} \right)^{.5} \times d_{ge} \qquad (1)$$

The variables $\rho_{particle}$ and ρ_{water} are the densities of the particle material and water, respectively, d_{ge} is the geometric particle diameter, and γ is a shape factor (1 for a sphere and almost always increasing for irregular shapes).[16]

Diffusion is the third and least probable mechanism for the deposition of particles > 1 μm, and is effectively negligible for particles > 3.5 μm.[9,13] This mechanism is controlled by the Brownian diffusion of suspended nanoparticles in the airways. It is the primary mode of deposition in the alveoli due to the limited convection of air in the tiny pores. This mechanism is only considered important

if it is found that particles deposit in the alveolus and are below a few microns in diameter.[13,17]

1.1 A Brief History of Pulmonary Drug Delivery

Pulmonary delivery stands out among the various delivery schemes for its fast onset of action and relative ease of administration.[18] Indeed, the pulmonary route has been employed since ancient times for the administration of various drug substances, but it has only recently gained attention in the modern medical field.[18] Various steroid based aerosols used to treat asthma were developed in MDIs and brought to the market in the 1950s.[19] After this time, developments in pulmonary delivery began to diminish, but DPIs were able to make their debut around 1970.[11]

DPIs were advantageous to MDIs because the patient did not have to coordinate his or her inspiration with the device actuation, drug was less likely to impact upon the patient's throat, and no environmentally harmful propellants were needed.[9,20] A major drawback with the performance of DPIs was that a portion of the inhaled particles would often get stuck in the upper airways due to particle agglomeration or insufficient aerosolization which caused inconsistent dosing.[9,11] Over the next twenty years, new designs were introduced to both improve the usability of the devices and increase the number of doses the DPIs could store.[11] Pulmonary delivery became increasingly attractive both to present

drugs locally to the lungs, as well as to deliver therapeutics through the lungs to the systemic environment without experiencing the effects of first pass metabolism.[9] Along these lines, pulmonary drug delivery is now increasingly seen as a viable strategy for treating a number of diseases such as lung cancer, primary pulmonary hypertension, cystic fibrosis, chronic obstructive pulmonary disease, emphysema, and tuberculosis.[10,21]

Pulmonary delivery vehicles may be composed of a variety of materials including; pure drug particles, nebulized liquid droplets, biodegradable polymers, etc.[22] For example, aerosolized and intratracheal bolus doses of surfactants, synthetic and natural, have been delivered to the pulmonary bed in treatment of various respiratory distress syndromes.[23,24] Synthetic surfactants consist primarily of dipalmitoylphosphatidylcholine (DPPC), while natural surfactants may be harvested from the bovine lung.[25] These surfactants may also be used in drug delivery formulations.[26] Experience has shown that, depending on the drug, the desired time of release and site of action, one delivery vehicle may be preferred over another.[27]

While device design was explored during the infancy of pulmonary drug delivery, material selection has recently received much attention. Biodegradable polymers have had a greatly positive impact in pulmonary medicine.[28] PLGA, poly (lactic-co-glycolic acid) is one such polymer that has been micronized for pulmonary delivery.[29] Lai *et al*., showed a therapeutic effect in using this polymer

to intratracheally deliver isoproteranol to achieve bronchodialation in serotonin challenged rats.[30] New studies have looked into PEG-based polymeric vesicles to overcome some of the limitations of PLGA based drug delivery.[31] PEG is slowly degraded via surface erosion kinetics as compared to the hydrolytic acid catalyzed bulk erosion of PLGA.[9,31] Chitosan is a polysaccharide, a sugar-based polymer, that has been employed in several pulmonary formulations to improve release kinetics and drug permeability.[32] As time continues, all of these technologies may be refined and used to improve pulmonary drug delivery.

1.2 Pulmonary Physiology and Molecular Transport

The lungs are dynamic organs that serve as the core of the respiratory tract in all species of land animals.[33] The respiratory tract contains a great number of different tissues and regions, each with unique structure and function. A diagram of these various regions is shown below.

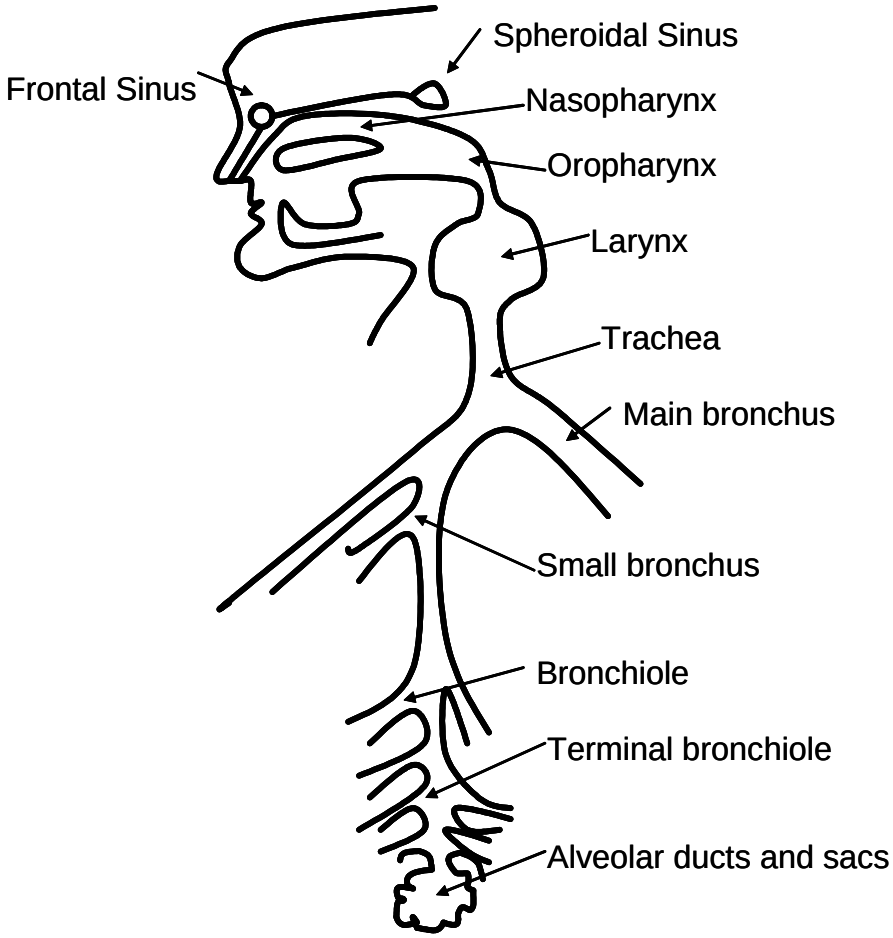

Figure 1.3 Diagram of the various structures within the human lung physiology. Adapted from Hillary, *et al.*, 2001.

Transport issues should be considered for the entire respiratory tract when designing a pulmonary drug delivery device. The various regions are composed of unique tissue structures that serve as barriers to drug delivery. If the cells on the surface of the airways are ciliated they may remove particles before drug can be dissolved to the mucosal layers. Epithelial cells equipped with a protective extracellular matrix and an increased number of tight junctions will prevent

transport of hydrophilic molecules. Hydrophobic molecules may pass through cell walls and into systemic circulation, but dense submucosal layers and a highly charged mucus layer may prevent this route of drug transport.

Aside from these barriers, drug entities delivered via the lungs are able to avoid first pass metabolism in the liver and this may increase overall bioavailability.[34] There is evidence that drugs containing an ester moiety may experience a pulmonary first pass effect due to enzymatic degradations via carboxylesterase isozyme, but this phenomenon is limited to specific drug types.[35] The respiratory system consists of three primary regions: the upper airways, the central airways and the peripheral airways. A more detailed depiction of some of the surfaces of these regions is shown in Figure 1.3.

The upper airways share regions with the gastrointestinal tract (mouth, oropharynx, larynx, and trachea). The pulmonary route literally begins at the mouth and leads to the throat.[1] These surfaces are composed of a non-keratinized epithelial layer with a saliva based mucus layer that interfaces with the air, and a mucosa layer between 0.5 and 0.8 mm in thickness.[9] The oropharyngeal region follows, which includes the oropharynx and the larynx (nasal anatomy in this region is omitted for brevity). Inhaled air then passes through the trachea. An image of this region is shown below.

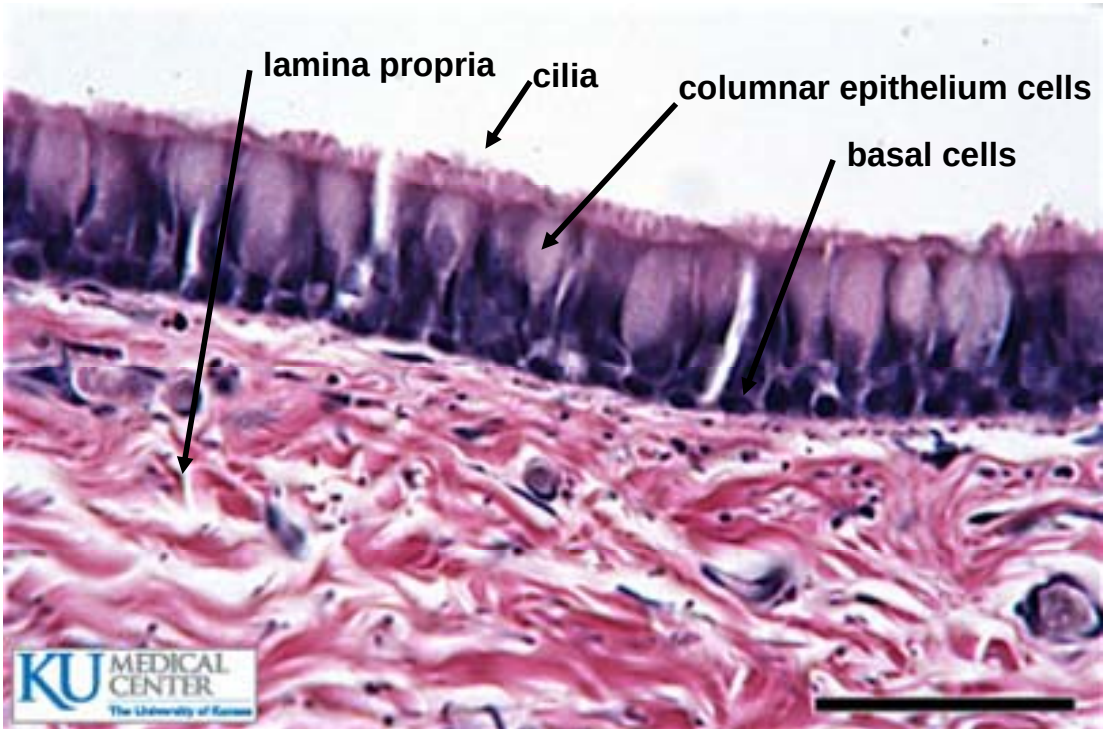

Figure 1.4. Histological section of the ciliated epithelial layer in the upper airways. Bar = 50 μm. Courtesy of KU Medical Center.

Figure 1.4 shows the typical ciliated morphology of the mucosal cells which facilitate mucociliary transport between this region and throughout the lung tissues to the terminal bronchioles. Particles with an aerodynamic diameter greater than 10 μm may be deposited in this region due to heavy impaction. This has been the case in early devices, and some studies have shown anywhere from 9 to 76% deposition in the mouth and throat for monodisperse aerosols.[36] Virtually no drug deposited here is able to transport through the cell layers before being swallowed or expectorated.

The next region is the central or conducting airways. This area consists of the lower trachea, main bronchus and the many bifurcations that make up the bronchiole tree (~23 in total). This region is not considered ideal for drug delivery as it contains a thicker, less penetrable epithelium that the distal branches and alveoli, and also contains cilia and a mucus layer which provide for constant mucociliary clearance from the walls of the bronchi, sweeping particles up to the trachea and down into the GI tract. An image of this region is shown below.

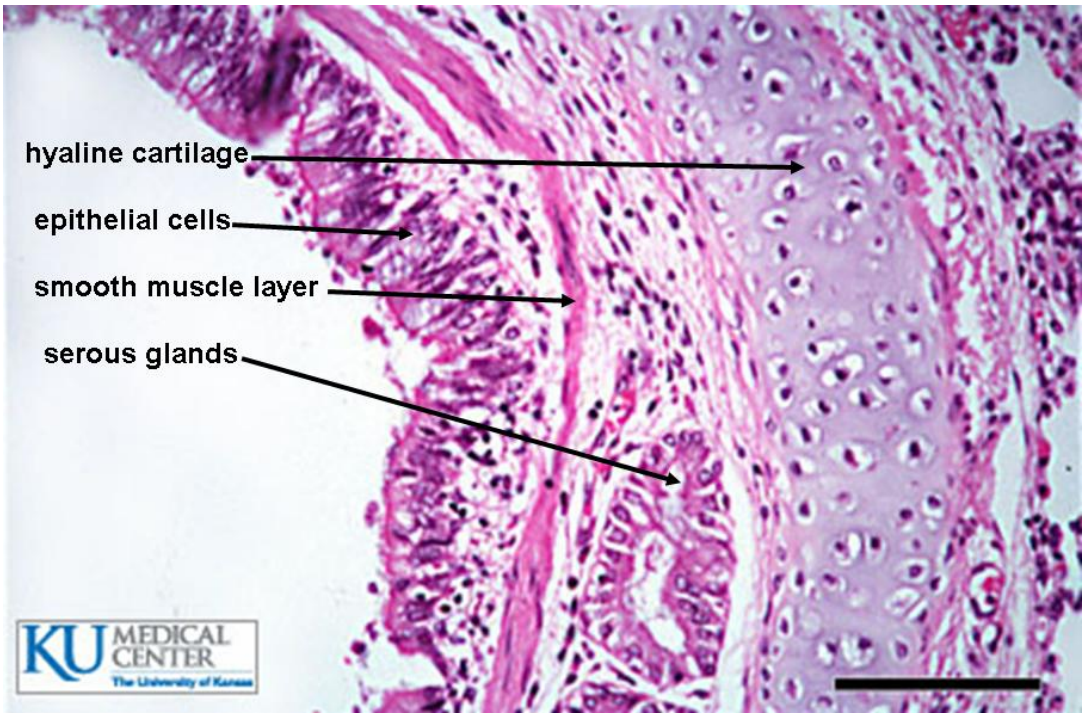

Figure 1.5. Histological section of the walls of a bronchus. Bar = 100 μm. Courtesy of KU Medical Center.

This region is primarily lined with ciliated and goblet cells. The goblet cells secrete components of the mucus layer along with the submucosal glands, and the ciliated cells provide for clearance. Serous, brush, and clara cells are also present

in small amounts. The surfactant that covers the mucus layer is provided by epithelial type-II cells. These are cuboidal pneumocytes which exclusively secrete a pulmonary surfactant consisting of a specific mixture of lipoproteins and lipids, the majority of which is phosphatidylcholine. The surfactant decreases surface tension upon exhalation and also helps reconstitute proper morphology upon inhalation.[9]

The final region of the airways is the peripheral airways, which consists of the terminal bronchi and the alveoli. This region is usually considered the optimal location for particle deposition, because it contains the largest surface area for molecular transport, a minimal surfactant layer to impede transport, the thinnest layers of epithelium to shorten transport events, and no ciliated cells. An image of this region is shown below.

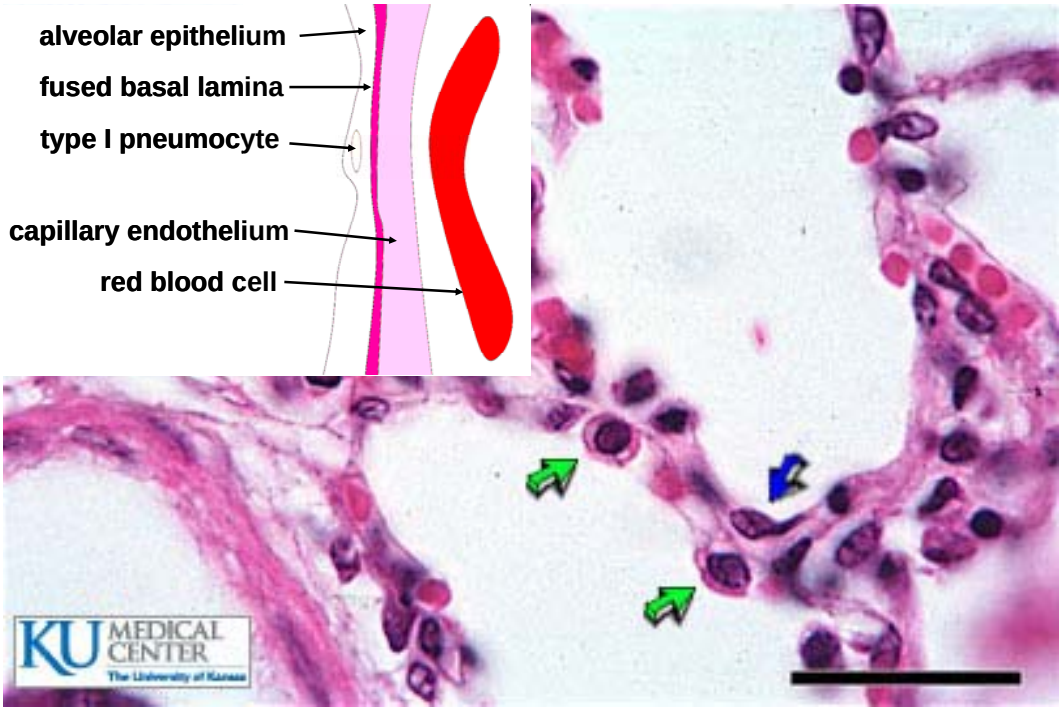

Figure 1.6. Histological section of the alveolar region in the human lung. Insert shows a schematic of the blood/alveolar interface. Blue arrows point to type I pneumocytes, green arrows point to type II pneumocytes. Bar = 30 μm. Courtesy of KU Medical Center.

This region is composed of type I and II pneumocytes. Type I cells compose about 33% of the cell mass, but they compose almost 93% of the alveolar surface. These cells are very thin, about 0.05 μm, and offer a direct route to the systemic circulation for gases. Type II cells are responsible for secreting the surfactant that regulates surface tension on the surface of the alveolar lumen. This layer interfaces with the endothelium of the blood capillaries via a fused basal lamina. This region can be as thin as 0.5 microns wide and primarily allows for rapid gas exchange between the airways and the blood, but it is also a target area for drug transport into the systemic environment.

The alveolar region contains macrophages which exist primarily to engulf and clear harmful particulates. Particles that are taken up by macrophages may endure one of several fates. Most often, they are transported to the terminal bronchioles, where they are then cleared via mucociliary clearance. Nanoparticles may also be carried though the alveolar epithelium and reach the lymphatic tissues in the interstitium. The particles are then translocated to the bronchial associated lymphatic tissue where they are released back into the upper airways for clearance via exhalation. This is a possible fate for deposited nanoparticles, and it yields clearance rates comparable to the mucociliary pathway for microparticles.[37] Particles that are able to reside in the alveolar region for a period of time may release their drug via particle erosion, particle degradation, and/or drug dissolution. Dissolved drug can then transport through the cell membrane or between type I pneumocytes, depending on hydrophobicity, and enter directly into the capillaries. These regions are shown in detail in Figure 1.6.

The pulmonary environment contains a range of fluid/fluid and fluid/solid interfaces in the course of drug transport.[33] These various interfaces include: air/surfactant interface between the bronchial/alveolar lumen and the mucus layer that covers the walls of the lumen,[38] particle/air interface between the surface of the drug particle and the air within the bronchial and alveolar lumen,[13] and aqueous/epithelial interface between the mucus layer and the walls of the lung epithelial cells that line the airways.[13,39,40] In the course of delivering drugs via the

pulmonary route, any of these interfaces may be of importance in considering efficacy of overall drug delivery.[9,13,39-41] Also, upon particle deposition there is a boundary between the particle and the mucus layer whereby drug release may be a major limiting kinetic event. Nanoparticles may be able to penetrate epithelial cell membranes, but the highly charged mucus layer may still provide a major barrier to their delivery.[42]

Many barriers exist when delivering drugs locally or systemically via the pulmonary route, and some have already been briefly mentioned. Poor deposition of particulates is a primary concern.[9] If particles are not able to be deposited into the pulmonary bed, they may deposit within upper airways such as the oropharynx, larynx, trachea and upper bronchioles.[9,41] If this is the case, it is likely that the drug will be cleared via the mucociliary clearance mechanism and be deposited into the stomach and degraded and/or delivered into the gastrointestinal tract.[5] If the drugs are able to deposit along the terminal bronchioles and within the alveoli then there is an improved probability for dissolution and adsorption. Hydrophobic drugs are typically poorly soluble in lung surfactant, though the mixture is more effective in solubilizing these drugs than a pure aqueous environment.[43] Hydrophilic drugs bear the opposite challenge. Even though they may readily disperse throughout the surfactant layers, they still may not be provided with a suitable paracellular pathway to the capillaries through the tight junctions of the epithelial barrier. The surface cells in this region

of the lungs are characterized by their lack of interstitial spacing between cells. Hydrophilic drugs do not transport directly through the cell layers because they do not interact with the fatty surfaces of cells. Delivery may be enhanced with mucoadhesive delivery vehicles,[26] or permeability enhancers.

1.3 Manufacturing Particulates for Drug Delivery

Popular methods to produce particles for drug delivery are usually characterized as top-down processes, while bottom-up processes mainly refer to nanoparticle fabrication via molecular self-assemblies.[44] Top-down processes include spray drying, emulsification, anti-solvent precipitation, Supercritical CO_2 precipitation, wet milling, jet milling, and grinding. Nanoparticles can also be produced using these processes. Rasenack *et al*., have reported the micronization of a host of anti-inflammatory drugs for pulmonary drug delivery using a controlled crystallization technique, and this may be considered a bottom-up process for micro or nanoparticle fabrication.[45]

One of the most well known methods for the production of particulate drug delivery vehicles is the formation of microemulsions and miniemulsions, where microemulsions generally refer to any liquid droplets that are stabilized against coalescence using surfactants with a size range between 1 and 1000 μm, and miniemulsions specifically refer to their nanosized counterparts with a size range between 1 and 1000 nm.[46] Miniemulsions have been shown to provide

'nanoreactor' systems for producing solid polymer nanoparticles.[46] An example is the emulsion polymerization technique whereby monomer is dissolved in a solvent and this dispersed phase is subject to shear along with a continuous phase, a surfactant, and an osmotic pressure agent, if necessary. The resulting nanosuspension is then allowed to polymerize and the solid nanoparticles are formed accordingly. The particles can encapsulate drug or bear it on their surface, depending on when the drug is introduced during the polymerization and the type of polymer synthesis routine such as: emulsification-evaporation, diffusion, solvent displacement, or salting-out.[47] Polymer nanoparticles, however, are used less often for pulmonary delivery.

Precipitation based methods have been used extensively for the production of drug particles. Solvent emulsification/evaporation methods refer to the formation of an oil/water emulsion that precipitates a solid suspension upon evaporation of the water immiscible solvent.[48] A similar method involves the virtually instantaneous precipitation of a solid suspension upon mixing of miscible solvents. The solid drug material is dissolved in a solvent, and it precipitates out when the solvent is mixed vigorously with an antisolvent.[49] The event may occur in the presence of stabilizers, which are shown to lower interfacial tension, increase nucleation rate and inhibit coagulation. The main controlling parameter in promoting nucleation and, thus, nanoparticle formulation is the degree of solute supersaturation in the antisolvent phase.[50] In contrast to mechanical milling

processes, antisolvent precipitation can offer control over morphology of the drug species. [51]

Supercritical CO_2 has been used as a solvent in the production of particulates suitable for drug delivery.[52,53] Several methods are employed for supercritical solvent processing including rapid expansion of supercritical solutions (RESS), gas antisolvent recrystallization (GAS), precipitation with compressed antisolvents (PCA), and still others with slight variations from these three.[52] Each is slightly different in setup, but all maintain the use of supercritical CO_2 to vary drug solubility with minor changes in pressure. RESS refers to dissolving the drugs in supercritical CO_2 and forcing the solution through a nozzle, thereby subjecting the fluid to a drop in pressure and the drug precipitates out in the form of particulates. This is a suitable method for drug with considerable solubility in the supercritical solvent.[54] GAS refers to expanding a drug/solvent mixture within a supercritical or condensed CO_2 bulk phase in a batch process. The new tertiary system yields much lower drug solubility than the initial solvent and particles precipitate out in solid form. When the drug/solvent mix is introduced via atomization it is known as PCA. If the CO_2 phase is supercritical, PCA is known as SAS or ASES.[52]

Spray drying is the common method for producing particulates for dry powder aerosol formulation. This process generally consists of atomizing a solvent suspension of drug and carrier into a hot air stream.[55,56] The atomization forms

nano and/or microparticulates and the solvent evaporates quickly into the air, forming dry powders. Spray drying can produce microparticles with geometric diameters ranging from microns to tens of microns, and composition can have a major effect on particle morphology.[57] There are some drawbacks to consider. Droplets that form at the nozzle usually form with a highly polydisperse size distribution. Resulting powders are equally polydisperse, and this may lead to poor deposition in the target airways. The use of caustic solvents and rapid heating at the air/droplet interface may lead to drug degradation. Lastly, this process generally requires large amounts of excipients to overcome the tendency for particle agglomeration upon rapid drying. These materials are not desired due to their added cost and potentially adverse side effects in patients.

1.4 Nanoparticle Formulations for Pulmonary Drug Delivery

Nanoparticles are rarely used on their own for pulmonary drug delivery, since these tiny particles fail to deposit and can be exhaled. Instead, they may exist as a component in a microparticulate system; either within or on the surface of a carrier microparticle or within a nebulized liquid droplet suspension.[58] There are a select few cases where nanoparticles were used independently as a pulmonary drug formulation. Videira *et al.*, performed rat studies on the uptake of solid lipid nanoparticles into the lymphatics.[59] These particles were shown to have mean diameters ranging between 218 and 220 nm after nebulization, and they exhibited

uptake into the regional lymph nodes. It was surmised that the mechanism of delivery was through phagocytosis via the alveolar macrophages, similar to ordinary particulate antigens.[59]

In another study, Zhang *et al.*,[60] studied the hypoglycemic response of rats with insulin nanoparticles delivered intratracheally. Briefly, 100 mg of dextran 70 was dissolved in about 9 mL of DI water and 100 μL of alpha-butylcyanoacrylate was added dropwise. The particle diameter was 254.7 nm with a polydispersity of 0.064. Glucose levels significantly decreased after administration of nanoparticle solutions directly into the trachea. The results showed the nanoparticles to be an efficacious delivery vehicle. The resulting particles exhibited comparable bioavailability to free insulin in solution and slightly lower bioavailability when compared to subcutaneous administration of insulin in solution.[60]

Nanoparticles may be used exclusively as a pulmonary delivery technique, but it may be expected that the successful application of free nanoparticles will be limited. Instead, there is much more research with regards to pulmonary administration of microparticulates.

1.5 Microparticle Formulations for Pulmonary Drug Delivery

Microparticluate drug delivery vehicles are diverse in morphology. Previously, PLGA nanoparticle agglomerates were produced that form microparticle sized dry powders suitable for pulmonary delivery.[61] This approach allows for the prospect of delivering drug loaded polymer nanoparticles directly to the alveolar space while also allowing for a porous morphology. Additionally, the use of two separate systems of nanoparticles in the microparticle formulation allows for potential bifunctionality of the overall delivery system. Combinations of sizes may allow for controlled release and drug combinations may easily be adapted into the formulation.

Initial techniques for producing microparticles as dry powders for pulmonary delivery involved jet-milling of the drug.[62] These particles were shown to bear flat geometries and subsequently high adhesion forces which made them difficult to disperse in the pulmonary airways.[63] Along with jet milling, ball milling was tested for powder formulation, with similarly limited success.[64] These processes involved high energy input that often led to reduced crystallinity of the drug and subsequent degradation.[65]

Spray drying has been shown to produce solid microparticulates suitable for pulmonary delivery.[6,66] Huang *et al.,* have used spray drying to produce chitosan microparticles encapsulating betamethasone as a model corticosteroid inhalation therapy.[57] As early as 1994, Chawla *et al.,* have used this method to produce

salbutamol sulfate drug microparticles for aerosol delivery.[56] Many other examples of this successful approach exist, but drawbacks are present. In the course of atomization and evaporation, particles are lost by adsorption to the walls of the air container, and they may also uncontrollably agglomerate.[67]

Lactose is used as a carrier particle with micronized or nanoparticulate drug particles adhered to its surface.[9,68] In the carrier particle strategy, drug microparticles and much larger (20 to 100 μm) lactose carrier particles are manufactured separately, usually via milling and spray drying, respectively, and subsequently mixed in the dry state.[69] Studies reveal that both lowering the size of the carrier particles, and improving their surface smoothness may improve aerosolization of the mixture.[68,70] More recent studies have shown that including a fraction of fine lactose particles, those with mean diameters less than 10 μm, can minimize the influence of carrier surface smoothness and particle size on the overall aerosolization, and thus performance may be improved.[71]

Supercritical CO_2 is often used to produce nanoparticles which are then incorporated into a carrier system. The solvent does work to produce microparticles, as well. Supercritical CO_2 was used in an aerosol solvent extraction system (ASES) to produce fluticasone proportionate microparticles for use in an MDI for the treatment of asthma.[72] The particles exhibited comparable flowability to the marketed formulation.

Finally, some lesser known methods have been employed for producing pulmonary microparticulates. Kwon *et al.*, have described a 'seed zone' method for producing micron sized insulin crystals.[73] This method takes advantage of insulin's variable solubility in the aqueous due to differences in pH. Briefly, the team dissolved insulin in low pH solutions (pH = 2.0) and subsequently increased the pH stepwise with additions of NaOH until they reached the 'seed zone' (pH = 10.5). Upon seeding the crystallization, the team then lowered the pH to 6.0 and stored the resulting microparticles. The resulting inhalable formulations exhibited suitable sustained release and particle sizes around 3 μm.

Concentrated efforts to produce suitable microparticles for pulmonary drug delivery continue to take place. Areas of exploration include novel changes to processing techniques, particle morphology, controlled release, and drug types. Microparticles are used for efficient deposition to the deep lung, but nanoparticles are popular for their increased dissolution kinetics primarily due to larger surface areas. A merging of these two morphologies would lead to potential improvements in particle deposition and drug dissolution. The following chapter investigates the controlled agglomeration of nanoparticles in colloidal suspension for the fabrication of pure drug porous microparticles for pulmonary delivery. A model drug, nifedipine, was used in the study due to its current lack of attention in pulmonary formulations despite its therapeutic effect in the pulmonary tissues.

Chapter 2: Nifedipine/Stearic Acid Nanoparticle Agglomerates for Pulmonary Delivery

Abstract

Dry powder formulations are of great interest in the field of pulmonary drug delivery. They provide advantages to traditional suspension and nebulized droplet formulations such as ease of administration and simple device design. Traditional powder formulations attempt to aerosolize solid microparticles and entrain them in the lungs during inspiration. Particles of 1-5 μm in size typically facilitate lung deposition, however particles of this size are too large to allow for enhanced dissolution kinetics. If nanoparticles were effectively delivered to these regions of the lung, enhanced dissolution may further improve drug bioavailability and efficacy. The aim of this study was to investigate the synthesis and performance of nanoparticle agglomerates in the formulation of micron sized particulates for aerosolized pulmonary drug delivery. Nanoparticles of the hypertension drug nifedipine were synthesized via known solvent/anti-solvent precipitation techniques. The resulting colloids were destabilized via ionic charge interactions using common salts at different solution molarities to achieve a final agglomerated nanoparticle size distribution suitable for pulmonary delivery of particulates. Agglomerated nanoparticle sizes were observed prior to lyophilization and powders were collected for further characterization. Performance of the final micron sized powders was found suitable for delivery of nifedipine to the deep lung and the constituent nanoparticle agglomerates revealed enhanced dissolution of the drug species.

2.1. Introduction

Pulmonary formulation of dry powder aerosols represents a rapidly growing sector in the field of drug delivery.[1] With characteristically fast onset of action, high bioavailability and relative ease of administration, pulmonary delivery of drugs presents potential advantages to many traditional dosage forms.[18] Nifedipine (NIF) is one such drug that bears complicated pharmacodynamics in the traditional oral dosage form. Nifedipine shows limited systemic bioavailability via the oral route due to a combination of enzymatic effects in the stomach and small intestine, primarily from P450 reductase and CYP3A mediated drug metabolism.[74] Though it is effective in easing symptoms of severe hypertension, it sometimes can be harmful due to aberrant dosing leading to elevated vasodilation and extreme hypotension.[75] Nifedipine is particularly useful in treating pulmonary hypertension, but hypotensive side affects hinder the drug in this case.[76] Given orally, the concentrations that are needed to achieve beneficial effects to the heart may cause unwanted side affects, including an increase in mortality rate for patients with coronary heart disease.[77] For these reasons, current oral formulations of nifedipine bear a largely untapped therapeutic effect that could be harnessed if it were consistently administered at lower dosages. Pulmonary administration of nifedipine is one such strategy that might alleviate the aforementioned difficulties.

Nifedipine is a dihydropyridine and resides in a class of calcium antagonists known as calcium channel blockers. The structure is shown in Figure 1.1. The site

of action is at the calcium channels residing on the surface of all cells and it primarily acts upon smooth muscle cells and heart muscle cells. Nifedipine is a weak acid (pKa = 3.93) and is recognized for its photosensitivity and very low solubility in water (~10 μg/mL in water at 37 °C).[78] Most drugs in the class of dihydropyridines bear similar physical and chemical properties to nifedipine, such as hydrophobicity and pyridine backbone.

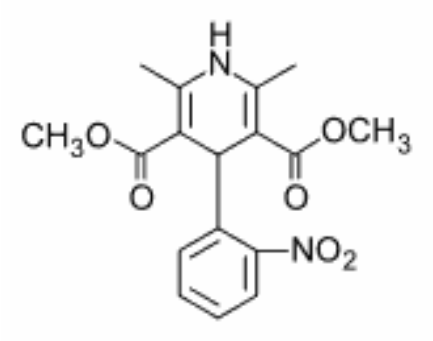

Figure 1.1. Chemical structure of nifedipine.

Evidence has shown nifedipine to be effective in the treatment of vasospastic angina, hypertension, aortic regurgitation, and chronic angina but not unstable angina.[79] This drug has shown a wide range of therapeutic effect, but often it is abandoned due to side affects such as pronounced hypotension, diarrhea, hepatotoxicity, mental confusion, and even death.[79,80] It has also been shown to cause gastritis in the GI tract.[81] These side effects, however, are primarily the result of excess drug in the dose as is required for current oral formulation. The common site of action for nifedipine is at the heart or the lungs, in the case of primary pulmonary hypertension. If nifedipine were able to be delivered via the

pulmonary route then it would be present at sufficient doses in the diseased tissue while avoiding many of its most unwanted side affects.

In the present study, the design and characterization of a dry powder aerosol of nifedipine is reported. A pulmonary formulation is envisioned as treatment of hypertension, primary pulmonary hypertension and/or chronic acute angina pectoris. Novel formulations of nifedipine have been investigated due to its poor solubility and limited bioavailability.[82,83] Few formulations, however, have employed the pulmonary route for nifedipine administration. To this end, nanoparticle agglomerates were synthesized via the destabilization of a suspension of stable charged nanoparticles (NP). Stearic acid allowed for stabilization of the resulting colloid, and facilitated destabilization with the addition of electrolytes. The resulting nanoparticle agglomerates demonstrated excellent aerosol properties and improved dissolution compared to micronized drug.

2.2 Materials and Methods

2.2.1. Materials

Nifedipine, stearic acid, and calcium chloride were purchased from Sigma Chemicals Co. USA and used as received in solid form. Ethanol 95% denatured, acetone electronic grade, and phosphate buffered salts were purchased from Fisher Scientific and used as received. Spectra/Por cellulose dialysis membranes (MWCO = 6-8 kDa) were purchased from Fisher Scientific. DI water was used throughout the study as obtained from a Millipore ultrapurification unit present on site.

2.2.2. Preparation of nifedipine nanoparticle suspensions

Nanoparticles were prepared by the rapid mixing of ethanol with dissolved nifedipine and stearic acid into a larger aqueous volume, known as a solvent/anti-solvent precipitation technique. In a common experiment, 10 mg of Nifedipine and 1 mg of stearic acid were completely dissolved in 1 mL of ethanol and allowed to stir overnight. This solution was added to 29 mL of cold deionized water via pipette injection under probe sonication (Fisher Sonic Dismembrator, model 500) at 60% amplitude for 20 seconds. The resulting colloid was then frozen at -20 °C and lyophilized, or stored in a 4 °C refrigerator until further processing into nanoparticle agglomerates. At this time, 3 mL was taken from the solution for sizing and imaging. All solution vials and reaction vessels were kept

covered from any light sources, as nifedipine exhibits considerable photosensitivity (~10% in 24 hours) from UV and visible light spectra.[84]

2.2.3 Nanoparticle characterization

Nanoparticle size, polydispersity, and zeta potential were all measured in solution directly after synthesis and prior to agglomeration by dynamic light scattering (Brookhaven, ZetaPALS). Zeta potential measurements were performed using 1 mM KCl solution. All measurements were performed in triplicate. Briefly, 1 mL of the solution was added to a standard cuvette and the remaining volume was filled with deionized water. Measurements were taken at 90 degrees to the incident light source while assuming a viscosity and refractive index of pure water. After arriving at a combined size, a second cuvette was filled with 1 mL of the colloid solution and the remaining volume was filled with KCl. A known voltage was then applied to this solution and data were analyzed via online software to determine the zeta potential of the particles in solution.

2.2.4 Preparation of nanoparticle agglomerates

Nanoparticle colloids were destabilized via ionic force interactions to produce stable agglomerates of nanoparticles. Briefly, 30 mL of the nanoparticle suspension was taken from refrigeration and solid salt crystals were added to 0.1 M. Directly after addition, the suspensions would be subject to vigorous mixing via probe homogenization operating at 20,000 RPM. Samples were left to sit at room temperature to allow complete agglomeration over 4 hours, and then transferred to a

-20 °C freezer before being lyophilized in a freeze dryer (Labconco, FreeZone 1). Some samples were allowed to settle for 24 hours and excess water was decanted prior to freeze drying. Drying continued for 36 to 48 hours to remove residual water. Lyophilized powder was stored in glass vials at room temperature until further characterization. Colloid stability was tested under a range of salt molarities and agglomeration behaviors were observed under all conditions.

2.2.5 Agglomerate characterization

Agglomerated nanoparticles were studied in solution and as a dry powder. After the agglomeration event was complete, a small volume (~3 mL) of the solution was analyzed using a Beckman Coulter Multisizer III with a 100 μm aperture tube. Data were collected until the output graphs showed a stable shape and particle counts were above 10,000. After lyophilization, particle yield was determined using the following equation.

$$Yeild = \frac{M_{powder}}{M_{initial}} \times 100 \qquad (2)$$

M_{powder} is the mass of solids retained after lyophilization, and $M_{initial}$ is the mass of solids introduced into the initial ethanol solution during nanoparticle fabrication plus the amount of salt added for agglomeration.

Dry powders of the nanoparticle agglomerates were analyzed by time-of-flight measurement using an Aerosizer LD (Amherst Instruments) equipped with a 700 μm aperture operating at 4 psi. For this step, 5 mg of the powder were added to

the aerosizer and data were collected until the output graphs showed a stable shape and the particle counts were above 10,000. Measurements were taken under medium shear and no regularization.

A cascade impactor was then used to collect data on powder performance (see appendix B). Briefly, eight filters were weighed and set onto collection plates which were housed within eight airtight stages arranged serially and stacked on a level setting. Air was then pumped through the stages at a rate of 30 liters per minute via a vacuum pump and about 10 mg of sample were introduced at the top of the impactor device. The powders were allowed to deposit amongst the stages for 20 seconds, after which time the air flow was stopped. Filters were then removed from the stages and weighed a second and final time. Cut-off particle aerodynamic diameters for each stage were provided by the manufacturer as follows: pre-separator – 10.00 μm, stage 0 – 9.00 μm, stage 1 – 5.8 μm, stage 2 – 4.7 μm, stage 3 – 3.3 μm, stage 4 – 2.1 μm, stage 5 – 1.1 μm, stage 6 – 0.7 μm, stage 7 – 0.4 μm and the final stage (stage 8) is intended to collect any remaining particulates, though complete entrainment is nearly impossible. Mass of material deposited on each stage of the impactor was determined by measuring the mass by differences of each of the filters placed on the stages. These respective masses were used to calculate the respirable fraction emitted via the following equation:

$$\%RF = \frac{\sum_{F}^{cutoff} m}{mtot} \times 100 \qquad (3)$$

Where %RF is the percent of respirable mass in the powder, F and cut-off designate the final and cut-off stage for the calculation, m is the mass on a given stage, and mtot is the sum of mass on all stages. The mass median aerodynamic diameter, MMAD, was obtained by a linear fit of a plot of the cumulative mass plotted as a function of the logarithm of the effective cut-off diameter, and recording the diameter at the midpoint of the curve fit.

Finally, the powders were characterized via two simple tests: a tap density test, and a test for angle of repose. The tapped and untapped (bulk) densities were determined by demarcating a small cuvette with known volumes, and then inserting a small mass of powder into the cuvette (bulk density) and tapping it vertically against a padded bench top 50 times (tapped density). The mass was divided by the initial and final volumes. From these values the Hausner ratio (tapped density / bulk density) and Carr's index (C_i) [(tapped density – bulk density) / tapped density X 100%] were also determined for each of the samples.[85,86] The angle of repose for each powder was measured via the fixed cone height method. Briefly, a glass funnel with an internal stem diameter of 5 mm was placed 1 cm over a glass slide. Particles were allowed to flow gently through the funnel until a cone was formed which reached the funnel orifice. The

angle of the cone to the horizontal was then recorded. This test was performed in triplicate for each sample.

2.2.6 Particle Imaging

Nanoparticles, microparticles and pure drug crystals were imaged via a scanning electron microscope. The samples were deposited onto mica slides in solution (or as received for the crystals) and allowed to evaporate overnight. These samples were then coated with gold palladium under an argon atmosphere using a gold sputter module in a high-vacuum evaporator. Samples were then observed for their surface morphology using a LEO 1550 field-emission scanning electron microscope.

2.2.7 Dissolution Studies

Dissolution of the nanoparticle agglomerates, nanoparticles, and pure drug were observed using a Shimadzu SPD-10A UV-Vis detector set for wavelength detection at 240 nm. The HPLC system consisted of a SCL-10A system controller, LC-10AT LC pump, SIL-10A auto injector with a sample controller, and CLASS VP analysis software. 45:55 (water:methanol) mixture buffered to pH = 4.5 was used as mobile phase. Flowrates in the column were adjusted to 2 mL/hr and all injections were taken at 50 μL. All studies were performed via a dialysis method in triplicate and sink conditions were maintained at a 30:1 volume ratio. Solutions were allowed to stir at 200 RPM without heating. The equivalent of 4 mg was introduced into dialysis bags with a molecular weight cut off of 6-8 kDa.

2.3 Results and Discussion

The properties of the nanoparticle and nanoparticle agglomerate samples are shown in table 2.1. Nanoparticle yields were considerably lower than agglomerate yields (~12% lower). This was mainly due to the tendency for nanoparticles to adhere to the surfaces of the collection vessels. Nanoparticles were more difficult then their agglomerates to transport after lyophilization, and this led to low yields.

It is hypothesized that the stearic acid in the formulation localizes at the surface of the nanoparticles arranging their carbon chains to the core of the particles while allowing the exposed carboxyl groups to hydrogen bond with the surrounding water molecules. The arrangement of stearic acid leads to higher negative surface charges on the nanoparticles which increased their stability in water and also may help form agglomerates upon addition of salt. This hypothesis was supported from the greatly reduced zeta potential of the stearic acid particles as compared with the pure drug nanoparticles (data not shown). Nifedipine is a characteristically non polar molecule, so any accumulation of charge on the surface of the nanoparticles may be attributed to the stearic acid. This reasoning is also aided by the observation that stearic acid is slightly amphiphilic, so it likely acts as a surfactant between the nifedipine and the surrounding water molecules after particle formation.

Table 2.1. Nanoparticle size, polydispersity, and zeta potential for an optimal formulation from an ethanol solution containing 1% w/v nifedipine and using stearic acid as a stabilizer in a ratio of 10:1 NIF:SA.

Particle property	Value
Effective Diameter (nm)	470 ± 40
Polydispersity	0.34 ± 0.1
Zeta Potential (mV)	(24) ± 6
NP Yield (%)	75 ± 5
Mean Agglomerate Dia. (um)	11 ± 6
Agglomerate Yield (%)	91 ± 4

It was observed that a main design constraint, nanoparticle size, could not be easily controlled by manipulating operating conditions during the formation of the colloid (data shown in Appendix A, Figures A2, A3). The rate of particle precipitation is strongly dependent on the relative solubilities of the drug in both phases (water and ethanol), and this effect was observed to dominate other potential factors in particle formation such as mixing energy and mixing time. As long as there was sufficient mixing of these two solvents, which was achieved via ultrasonication at low to moderate amplitudes, the nucleation and growth kinetics led to submicron particle sizes. However, if solutions were injected with too much drug, particle crowding would cause uncontrolled agglomeration and eliminate colloidal stability.

In designing the formulation, it was of great importance to control the surface charge of the nanoparticles. This is quantified as the zeta potential, shown in the Table 2.1. Charged particles are able to interact across long distances via

electrostatic forces.[87] Stearic acid was used to stabilize nifedipine nanoparticles. Stearic acid is found in the surfactant layer that rests above the lung epithelium in small amounts, is solid at room temperature, amphiphilic, and has also exhibited a small penetration enhancing effect for specific drug types.[88,89] Solidity at room temperature is particularly important to ensure solid morphology of the final powders. Also, the amphiphilic nature ensures that the molecule may act as an interface between the nifedipine and water phases.

Table 2.2 revealed flowability characteristics for three samples: stock nifedipine, nanoparticles and nanoparticle agglomerates. These data helped elucidate the bulk powder property differences between samples. Interesting points were observed, such as the large angle of repose for the nanoparticles, the decrease in density of the unprocessed drug with respect to the nanoparticles and of the nanoparticles with respect to the nanoparticle agglomerates, and the increasing Carr's index between the processing steps. A large angle of repose for the nanoparticles was probably the result of strong adhesion forces between particles, and specifically between nanoparticles and larger agglomerates in the bulk mixture. The stock drug showed some ability to pack, and this is revealed as the difference between bulk and tapped densities. Carr's flowability index provides a general indication of interparticulate forces.[27] As the index increases, the differences between bulk and tapped densities increase. This equates to a greater degree of interparticulate forces in the sample and generally poor

flowability. The data showed that the nanoparticle agglomerates yielded the highest Carr's index. However, these indices are not an absolute measure of the performance of a powder. Indeed, good flowability does not equate directly to enhanced aerosolization. The results indicated poor flowability for agglomerates, but further data revealed that the agglomerates were able to sufficiently aerosolize for pulmonary drug delivery.

Table 2.2. Flowability parameters for three samples: stock nifedipine as received, nifedipine/stearic acid nanoparticles and the corresponding nanoparticle agglomerates.

Sample	Stock Nifedipine	Nif/SA NP	Nif/SA Agglomerates
Bulk Density (g/cm^3)	0.9 ± 0.2	0.10 ± 0.01	0.07 ± 0.02
Tapped Density (g/cm^3)	1.0 ± 0.3	0.12± 0.01	0.09 ± 0.01
Carr's Index	10 ± 0.8	17 ± 1.0	25 ± 2
Hausner Ratio	1.1 ± 0.01	1.2 ± 0.2	1.3 ± 0.3
Angle of Repose (deg)	50 ± 1	77 ± 2	58 ± 4

The decreasing densities were congruent with other data such as the SEM images in Figure 2.1. The unprocessed drug was composed of large faceted solids resembling crystals greater than 100 μm. This macrostructure led to the high bulk density observed. The agglomerate images indicate a semi-porous structure and this probably led to the lower densities for the processed particles. Also, large arrays of agglomerates were shown to be consistently under 10 μm (Figure 2.1b). The monodisperse distribution indicates successfully controlled agglomeration.

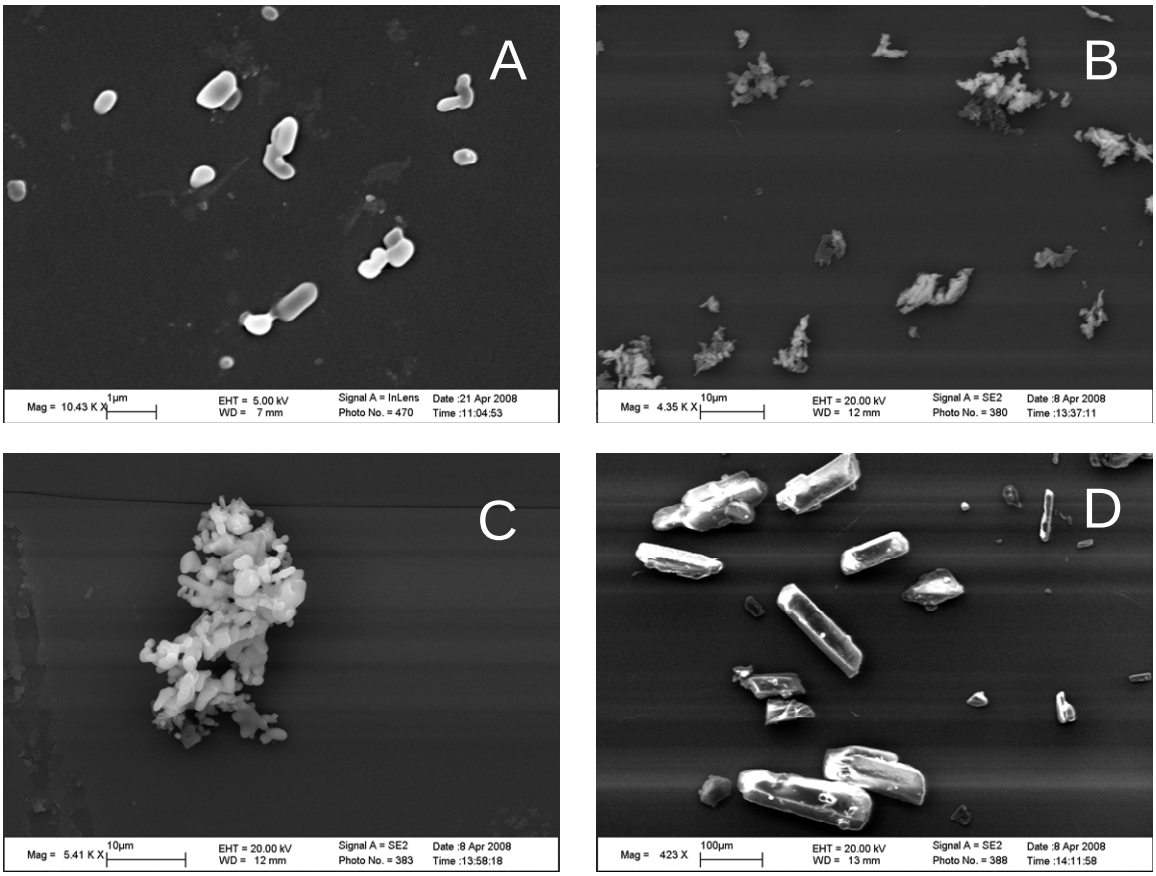

Figure 2.1. A collection of SEM images for nanoparticles (A), nanoparticle agglomerates with 1:1 salt addition (B), close up of a single agglomerate (C), and pure nifedipine crystals as received (D). Scale bars are 1, 10, 10, and 100 μm, A-D.

To begin characterization of the final powders, particle samples were tested on an aerosizer and a multisizer test their aerodynamic and geometric diameters, respectively (Figure 2.2). The multisizer data were collected in solution, and were important at this stage in the synthesis to verify the agglomeration event since it is well known that particles can agglomerate upon lyophilization. The samples revealed a fairly monodisperse distribution of sizes between about 2 and 20 μm,

with an average diameter of about 10 μm. More so, the data revealed very stable microstructure in the nanoparticle agglomerates. Their distributions were barely altered after intense homogenization, and the curves maintain their overall shape (Appendix A, Figure A2). Aerosizer data revealed a more monodisperse size distribution and a lower mean diameter.

The relationship between aerodynamic diameter and geometric diameter may be recalled from equation (1). The variables are arranged so that if the particle density is lower than that for water, then the aerodynamic diameter will be some fraction of the geometric diameter. Also, irregularly shaped particles yield a shape factor greater than one which will lead to the aerodynamic diameter being some fraction of the geometric diameter. In the case of our agglomerate samples, the geometric diameters were shown to be much larger, on average, than the aerodynamic diameters. For the sample shown in Figures 2.2, the average geometric diameter was about five times larger than the average aerodynamic diameter. Comparing these graphs offered a consistent confirmation that the particles were porous. The difference between particle distributions for the aerodynamic and geometric measurements suggested that the particles have excellent aerodynamic properties.

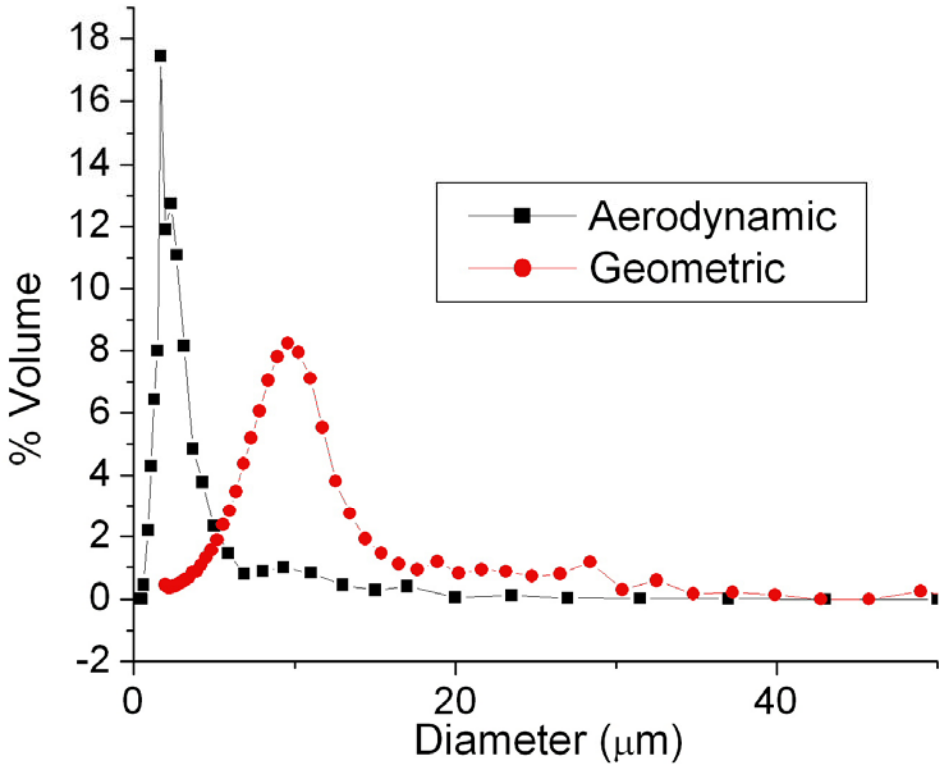

Figure 2.2. Aerodynamic and geometric diameter size distribution for a sample of nanoparticle agglomerates.

SEM micrographs from Figure 2.1 revealed the morphology of nanoparticles, nanoparticle agglomerates and pure drug. Images helped validate that nanoparticles agglomeration led to microparticle formation, since the images clearly indicated assemblages of nanoparticles. Wastewater treatment studies have shown that colloidal particles will agglomerate due to van der Waals forces, and that electrostatic forces are essential to avoiding this agglomeration.[90] These studies provide an ample background for gaining insight into colloidal

destabilization. The colloids, studied here, required simple charge neutralization to cause this agglomeration to occur. It is not surprising that the addition of electrolytes in the form of sodium chloride caused nanoparticle agglomeration, since stearic acid formed only a weakly negative surface charge to stabilize the nanoparticles. The mechanism has also been shown to benefit from anion presence, which further justifies the use of NaCl.[90]

The nanoparticle SEM images in Figure 2.1 showed a somewhat elliptical morphology with an average diameter somewhere below one micron, but not as small as 100 nm, which was consistent with DLS data. The nanoparticle agglomerate images revealed a highly textured morphology, with many small and similarly shaped protrusions from the surface. These features were indicative of the mechanism behind particle formation, as they were probably the result of nanoparticles grouped together during the agglomeration step. Also, we can see a somewhat porous assembly (Figure 2.1c). In comparison, the stock drug was shown to bear a highly faceted structure, and particles resembling crystals larger than 100 μm were observed. This faceted morphology was not observed in any of the other images, thus suggesting a possible change in overall crystallinity.

DSC thermographs were used to investigate the effects of processing on drug morphology, and to verify the overall content in each of the formulations. Both stearic acid and nifedipine exhibited sharp endothermic troughs where they undergo a melting phenomenon upon heating (Figure 2.3). Endothermic troughs

at the nifedipine and stearic acid location show up in all the graphs; however, their extent and exact shape undergo changes. Firstly, it can be seen that the area between the curves and the baseline decreased for all processed samples. This is probably due to the increased surface area and faster heating of smaller particulates. Overall heating requirements were calculated using a peak integration method (Table 2.3). Processed samples all showed lower heating requirements on a per mass bases compared to the stock materials, which was consistent with more efficient heating of smaller particles. The data showed peak locations close to the original locations in the stock material, verifying the samples composition. The heating requirements for any of the peaks were far lower than those for typical ethanol evaporation (heat of vaporization = 877 J/g), so we may conclude that negligible solvent was present in the processed particles.

Table 2.3. DSC peak integrations for stock nifedipine, stock stearic acid, NIF nanoparticles, NIF/SA nanoparticles and NIF/SA agglomerates.

Sample	Peak location (°C)	Peak area (J/g)
Nifedipine	174	121
Stearic acid	76	245
NIF nanoparticles	150	30
	156	28.8
NIF/SA nanoparticles	67	24.2
	152	32
	160	38.8
NIF/SA agglomerates	67	9.1
	163	36.3

It is worth noting the changed shape of the nifedipine peak for both nanoparticle samples, which revealed an exothermic peak indicative of a crystallization event, or some other energy yielding phenomenon (Figure 2.3). It may be hypothesized that the peaks result from a morphology change in the processed nifedipine upon heating, and this may have occurred if the nifedipine was in an amorphous state beforehand. The exotherm is not present in the agglomerated sample, so perhaps the drug already reconfigured during or after the agglomeration step. No other theory for this exothermic behavior has been surmised thus far. But, it is certainly not an interaction between the nifedipine and the stearic acid, since it appears for the pure nifedipine nanoparticles as well.

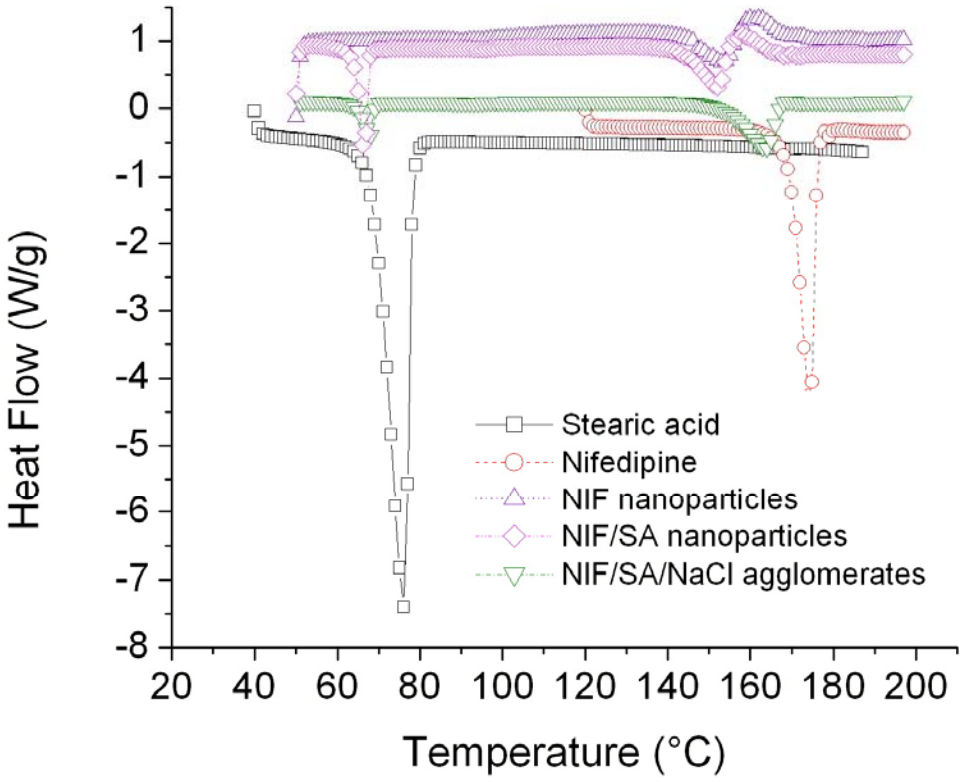

Figure 2.3. Differential scanning calorimetry outputs for stearic acid, nifedipine, pure nifedipine nanoparticles, nifedipine/stearic acid nanoparticles, and nifedipine/stearic acid/NaCl nanoparticle agglomerates.

Dissolution studies were conducted to measure the rate of nifedipine dissolution from the various forms of processed drug (Figure 2.4). Drug was mostly dissolved from nanoparticle and nanoparticle agglomerate samples within 10 hours. In the case of stock nifedipine, the kinetics slowed and less drug was dissolved throughout the experiment compared to the other samples. The nanoparticles released the most drug content in the allotted time. This is to be

expected as their smaller size allows for a greater surface area and faster dissolution to take place. The nanoparticle agglomerates dissolved faster than the stock drug by a considerable margin, but not as quickly as the nanoparticle suspension. The comparative dissolution rates indicated that dissolution rate increased for decreasing particle sizes. This behavior may also allude to improved dissolution characteristics of the agglomerates in the deep lung, though it was noted that the aqueous solutions used in the dissolution study may not sufficiently represent the environment within the lungs.

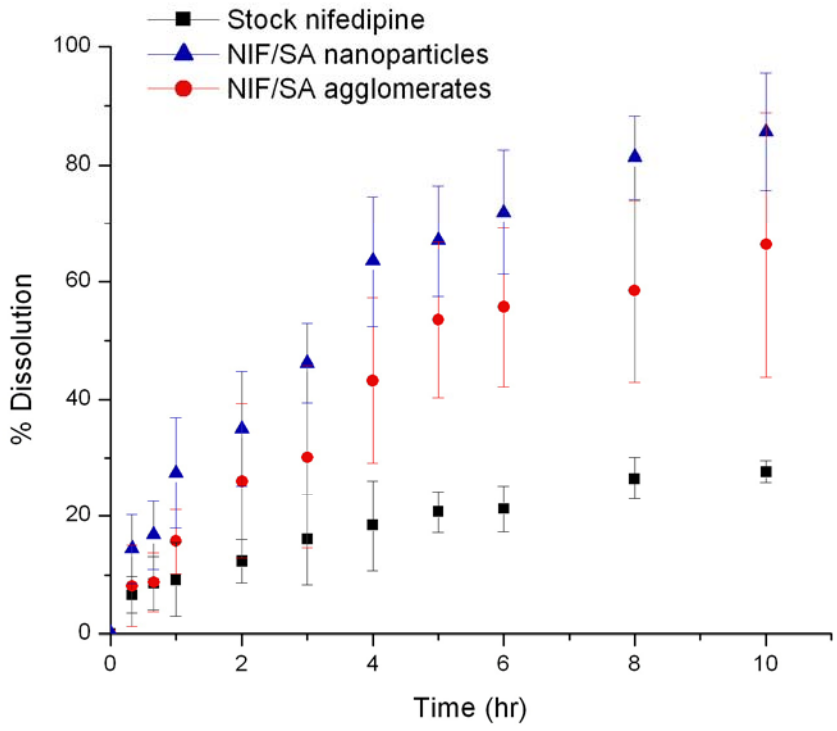

Figure 2.4. Percent drug dissolution versus time for the nifedipine/stearic acid nanoparticles, nanoparticle agglomerates, and stock nifedipine as received.

Particle size was shown to affect the overall rate of particle dissolution (Figure 2.5). Dissolution data was fit for first order kinetics, using the general first order rate equation shown below.

$$\frac{d(C)}{d(t)} = k \times C \qquad (3)$$

Where C is the concentration of undissolved drug, k is a rate constant and t is time. The equation can be solved for the single boundary condition where no drug is present in solution at t = 0 to yield an exponential function. This function was fit against all dissolution data to get rate constants for each sample. The data revealed that dissolution rate was inversely proportional to particle size. The rate was linear to the log of particle size, which is expected since the increasing size has an exponential effect on the available surface area for particle dissolution.

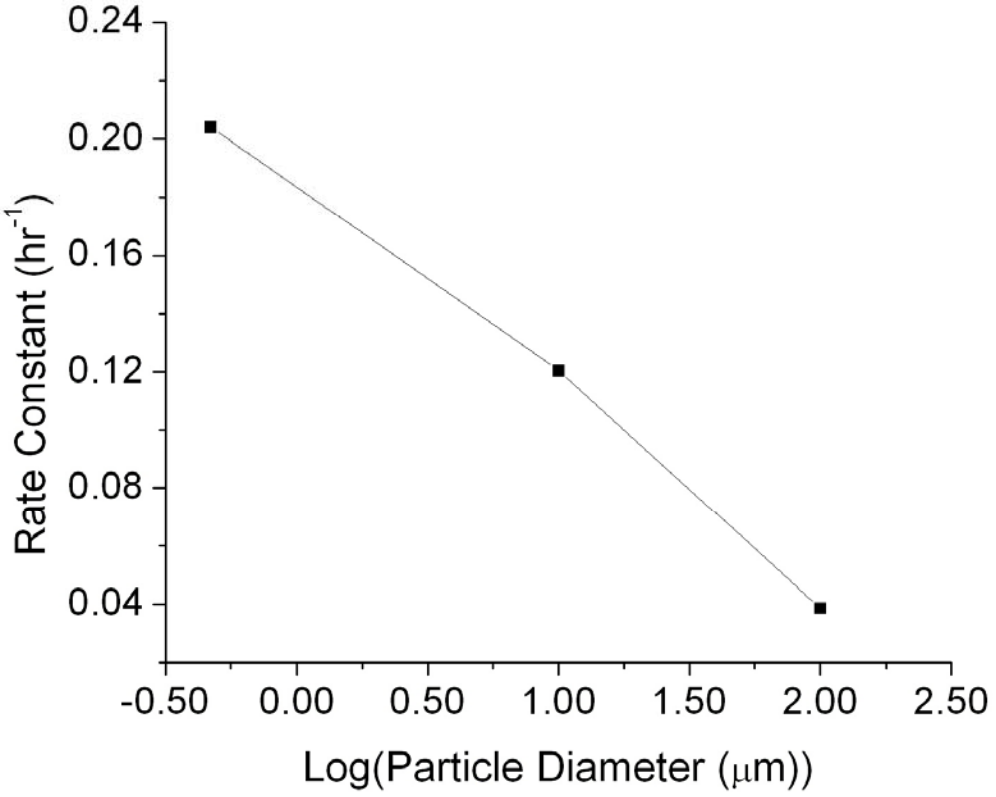

Figure 2.5. First order rate constants versus the logarithm of particle diameter for three samples: stock nifedipine, NIF/SA nanoparticles and NIF/SA agglomerates.

Nifedipine is photosensitive, and has also shown to degrade spontaneously in solution.[91,92] Although careful precautions were taken during sample preparation and dissolution studies, it was possible that portions of the total nifedipine mass degraded over time and the degraded species did not elute from the chromatography column with the native species. Alternate peaks aside from our characteristic peak were observed and identified as the byproducts of nifedipine degradation. These peaks increased in area as the studies reached their final time

points (data not shown); however, aberrant peaks only represented a small fraction of the dissolved drug at any given time point (~1-5%). They were included in computing the overall concentration of drug in solution. This was done to ensure that all dissolved drug was accounted for, and that kinetic data was minimally skewed due to species degradation throughout the experiment.

Finally, cascade impaction studies were performed to formalize powder characterization for pharmacological formulation characterization. The cascade impactor is a well known instrument initially designed in the 1950's for simulating aerosol performance in the human lung. The stages are set up so that each of them (0-8) represents deeper penetration into the lung. Particles of smaller sizes are not able to maintain their trajectories as the flowrate increases between stages. As a result, they impact upon the filter set on top of the next stage. A more in depth view of the device can be found in Appendix B. Data are summarized in Figure 2.6 and table 2.3.

Table 2.3. Cascade impaction results of three samples types: stock nifedipine as received, nifedipine/stearic acid nanoparticles and the corresponding nanoparticle agglomerates. EF% is the emitted fraction percent, RF% is the respirable fraction percent, and MMAD is the mass median aerodynamic diameter.

Cascade impaction data		Formulations		
		Pure	NP	Floc
EF%		85 ± 12	93 ± 6	91 ± 4
RF%	5.7 <	48 ± 4.1	84 ± 0.1	94 ± 1
	3.3 <	2.5 ± 1.5	84 ± 0.7	84 ± 4
MMAD		4.8 ± 0.6	1.8 ± 0.2	1.4 ± 0.1

The mass separation onto different stages revealed different behaviors for each of the samples. The pure drug mostly deposited in the earlier stages, 1-3. These stages represent the pharynx and primary bronchi and so it may be assumed that these powders would not enter the lungs whatsoever. The dried nanoparticles showed the bulk of their deposition between stages 5-7 and these represent the terminal bronchiolar and alveolar regions. A significant subpopulation of the nanoparticle sample deposited in stages 1-3, suggesting the present of large nanoparticle agglomerates as a result of the drying process. The nanoparticle agglomerates showed similar deposition patterns, but deposited strongly at the terminal bronchioles. Studies have indicated that this is an effective region for drug delivery.[93]

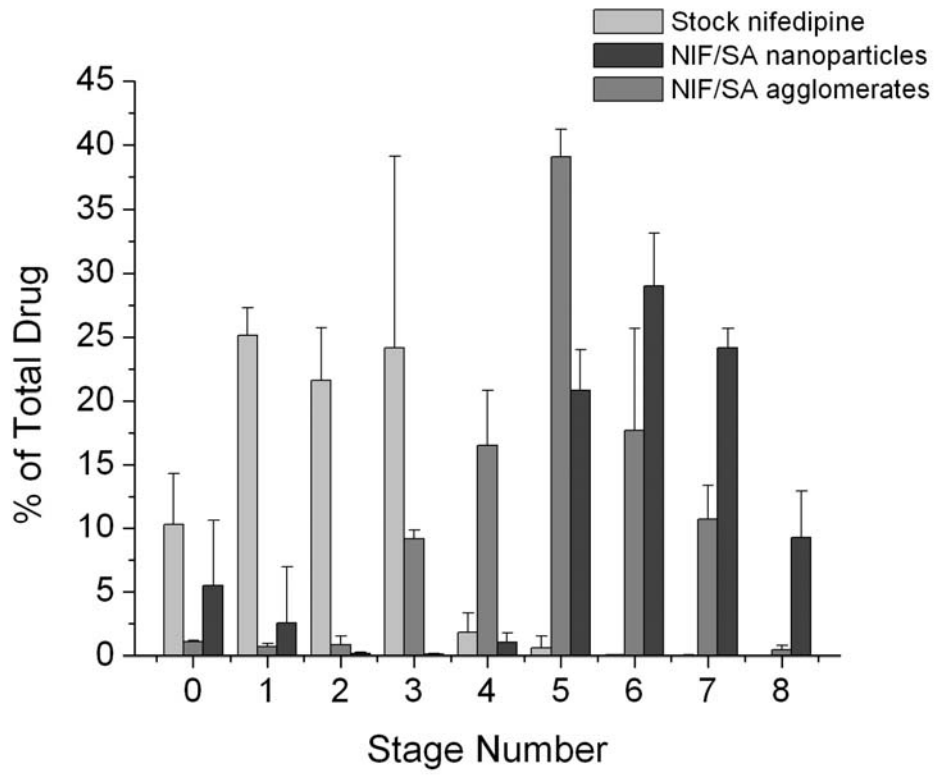

Figure 2.6. Cascade impactor readings for nifedipine/stearic acid nanoparticles, nanoparticle agglomerates, and drug as received. Data is represented as a percentage of mass deposited on each stage number within the cascade impactor.

From the data, it appeared that both the nanoparticle samples and their corresponding nanoparticle agglomerates were able to deposit efficiently to the lungs. The primary reason for this similarity, given different processing steps, is that the stearic acid-modified nanoparticles uncontrollably agglomerated upon lyophilization and hence revealed similar deposition behaviors. Also, the nanoparticles appeared to be depositing in the deepest regions of the impactor, but these particles may be quickly exhaled in a clinical setting, since deposition in the

alveolus often requires breath holding.[14] The agglomerated particles may bear further advantages to the nanoparticle formulation simply because of the ability to harvest them directly from solution. Via a combination of particle separation and drying, nanoparticle agglomerates may be isolated as a dry powder at a fraction of the cost of nanoparticles via lyophilization. Finally, the cascade impaction data (table 2.3) showed the nanoparticle agglomerates outperforming both the pure drug and the nanoparticle powders in all fields except for fraction emitted. The nanoparticle agglomerates showed an exceptional respirable fraction above 5.7 μm at 94.5% while the nanoparticles only presented 84.4% respirable at or below this diameter cutoff. Nanoparticles and nanoparticle agglomerates showed comparable mass median aerodynamic diameters, which, again, likely results from uncontrolled agglomeration of the nanoparticles during lyophilization.

2.4 Conclusions

Stearic acid stabilized nanoparticles of nifedipine were synthesized via solvent precipitation in an aqueous solution. These colloids were destabilized using salt at specific molarities to induce particle agglomeration and subsequent microstructure formation. Nanoparticles and nanoparticle agglomerates revealed enhanced dissolution kinetics when compared to the stock drug. The nanoparticle agglomerate dry powders exhibited flowability characteristics and size distributions suitable for pulmonary drug delivery. Future work should focus on deducing the crystallinity of nifedipine at the various stages of processing, and performing in vivo studies to compare the effectiveness of the agglomerated powders with pure nanoparticles and stock drug as a dry powder formulation for pulmonary delivery.

Appendix

A. Preliminary Investigations

Throughout the course of preparing samples for the prepared study in chapter 2, data were collected to help optimize the formulation and gain understanding of the processes at work. The dynamics of nifedipine nanoparticle and nanoparticle agglomerate synthesis were elucidated from these tables and figures. It is shown from table 3.1 that a range of nanoparticle sizes (200 to 700 nm) and surface charges (-20 to -35 mV) may be achieved through various processing conditions. All data in this table were obtained with ethanol as solvent and stearic acid as stabilizer.

Table A1. Nanoparticle size, polydispersity, and zeta potential under various operating conditions. Drug/acid is the ratio of mass of drug to the mass of stearic acid used in solution. Ethanol and Water refer to the volumes of both phases in the nanoparticle processing step. Son. time is the mixing time.

Sample	Size (nm)	Polydispersity	Zeta (mV)	Drug/acid	Ethanol (ml)	Water (ml)	Son. time (s)
A	235	0.03	-20.9	50.0	1.5	30	90
B	260	0.01	-27.4	10.0	1.5	25	90
C	263	0.24	-30.4	0.7	5.0	50	60
D	264	0.51	n/a	6.0	5.0	50	120
E	308	0.26	-19.7	5.0	1.5	25	60
F	318	n/a	-46.6	0.3	5.0	50	60
G	323	n/a	-33.6	0.6	5.0	50	60
H	336	n/a	-34.4	0.6	5.0	50	60
I	472	0.15	n/a	6.0	1.0	50	20
J	584	0.01	n/a	6.0	1.0	25	60
K	598	n/a	n/a	6.0	0.1	25	40
L	635	0.46	n/a	6.0	5.0	10	60
M	653	0.23	n/a	6.0	0.1	50	60

Nanoparticle formation does not show immediate dependence on either sonication amplitude or sonication time (tables A2, A3). However, it should be

noted that both tests were carried out while holding all solution variables constant (solvent/anti-solvent volumes, drug concentration in the solvent phase, drug/acid ratio). Further experiments may have shown stronger sonication amplitude and time dependencies if solutions were prepared under different concentrations. Even so, the final synthesis routine probably would not have changed since solution variables were chosen based on a number of reasons. The drug/stearic acid ratio was minimized to reduce dosing volumes and maintain pure drug morphology. The drug concentration in the solvent phase and the solvent/anti-solvent volumes were maximized to make the synthesis scheme cost effective. That is, lower concentrations would lead to high processing volumes and an increased energy cost. It remains for future work to compile a comprehensive report of the particle size and zeta potential dependencies under a comprehensive range of operating conditions.

Table A2. Particle sizes under a range of sonication amplitudes. W/O = 29, D/A = 1, Vtot = 30 mL, Prepared with 1% nifedipine in ethanol and stearic acid as a stabilizer.

Amplitude (%)	Effective Diameter (nm)	Polydispersity
10	630	0.10
20	700	0.30
30	950	0.30
40	1060	0.01
50	1050	0.20
60	1300	0.01
70	690	0.35

Table A3. Particle sizes under a range of sonication times. W/O = 60, D/A = 10, Vtot = 30 mL, prepared with 1% nifedipine in ethanol.

Time (seconds)	Effective Diameter (nm)	Polydispersity	Zeta Potential
5	534 ± 28	0.09	(14.3) ± 0.82
10	507 ± 39	0.15	(12.4) ± 0.69
15	553 ± 16	0.16	(15.6) ± 1.2
30	507 ± 20	0.18	(17.6) ± 2.1
60	495 ± 50	0.26	(15.6) ± 0.64

Data suggested that stearic acid concentration may have a small effect on nanoparticle characteristics (table A4). It seems that increasing the concentration of the acid from 0.1 to 1 weight percent may slightly increase the size of the nanoparticle, as well as increasing the surface charge. Both of these outcomes follow intuitively. With more of the lipid present on the surface, the particles will be larger, and there will be a greater tendency for the carboxyl chains to be exposed to the environment which will increase the negative charge. The added material does not lead to an increased number of small particles possibly because stearic acid has no effect on the particle nucleation rate due to its higher water solubility compared to nifedipine.

Table A4. Nanoparticle characteristics after preparation with a range of stearic acid (SA) concentrations in the solvent phase. Negative values are in parenthesis.

Sample	Effective Diameter (nm)	polydispersity	Zeta Potential
0.1 % SA	235 ± 8	0.03	(20.9) ± 3.0
0.5 % SA	259 ± 3	0.01	(27.38) ± 2.2
1 % SA	308 ± 8	0.25	(29.67) ± 1.2

Acetone was tested as a possible solvent phase during nanoparticle fabrication (table A5). Nifedipine is much more soluble in acetone than it is in ethanol, so it was possible to use far less solvent in making the particles. In these experiments, a tenth of the solvent (100 μL) was used in comparison to the ethanol experiments, but the same mass of nifedipine was prepared. Nanoparticles were successfully generated, and it can be seen that their sizes decreased from almost 700 nm to 430 nm when increasing anti-solvent phase from 10 to 50 mL water.

Table A5. Nanoparticle properties for suspensions created using acetone as a solvent phase. Sample names refer to the amount of anti-solvent phase (10,25 and 50 mL).

Sample	Effective Diameter (nm)	polydispersity
NP 10ml	671 ± 160	0.30 ± 0.1
NP 25ml	658 ± 130	0.30 ± 0.2
NP 50ml	431 ± 18	0.30 ± 0.01

Similar dependencies on the relative amounts of solvent and anti-solvent phases were seen for ethanol based formulations (Table A6). In these experiments, the anti-solvent phase was kept constant (50 mL) and a solution of nifedipine and stearic acid in ethanol at (1% and 0.1%, respectively) was added in varying amounts (1, 2.5 and 5 mL) under sonication. The data showed that increasing ratio of solvent to anti-solvent increased the size of particles formed, and microparticles formed as this ratio increased.

Table A6. Nanoparticle properties for suspensions created using ethanol solutions under a range of volumes. Sample names are designated according to ethanol volume used (1, 2.5 and5 mL).

Sample	Effective Diameter (nm)	polydispersity
NP 01ml	485 ± 9.5	0.3 ± 0.04
NP 25ml	1060 ± 290	0.3 ± 0.04
NP 50ml	2770 ± 160	0.5 ± 0.15

It was noticed during experimentation that the solutions were less stable than their ethanol based counterparts. Acetone solutions tended to show foamy residues on their surface, while ethanol solutions are typically homogenous and translucent in appearance. Also, particle sizes for the acetone preparations increased over short periods of time probably due to uncontrolled agglomeration (data not shown). One potential reason this happens is because nifedipine is used in such high concentrations with acetone. Solutions were prepared near the solubility limits for both solvent phases (17 mg/mL NIF in ethanol, 250 mg/mL NIF in acetone). The higher concentrations used in the acetone solutions may have resulted in nanoparticles forming in closer proximity upon mixing of the solvent and anti-solvent leading to their increased tendency to agglomerate.

Multisizer outputs for several different agglomeration routines were obtained (Figures A1 through A4). The figures showed aspects of the agglomeration for three different salts: NaCl, $CaCl_2$, and $MgSO_4$. Other salts were investigated to gain insight into the flexibility of the process. The three salts successfully agglomerated the nanoparticle suspensions, but discrepancies in these graphs

indicated that some salts were better than others in forming nanoparticle agglomerates.

Figures A1 and A2 revealed the effects of homogenization on agglomerate samples. After stable agglomerates are formed it is not possible to break them into their constituent nanoparticles via homogenization. This is evident in Figure A1 because the size distributions maintain mean diameters all around 5 μm following homogenization at various speeds. The Sample in Figure A2 undergoes a less drastic change in its size distribution after homogenization. This may possibly indicate an improved stability for the agglomerates, given that all homogenization regimes were essentially the same.

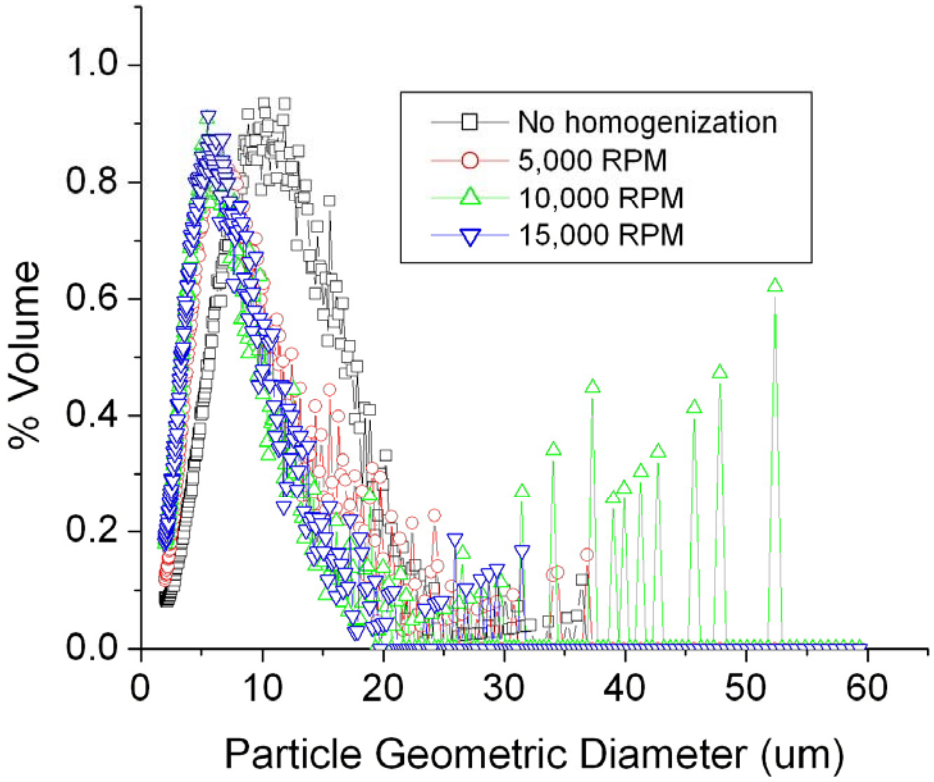

Figure A1. Particle size distributions for an agglomerate sample and portions of the sample after three homogenization regimes. Portions of a sample were subject to increasingly powerful homogenization regimes from 5, 15, and 25 kRPM for 30 seconds, respectively.

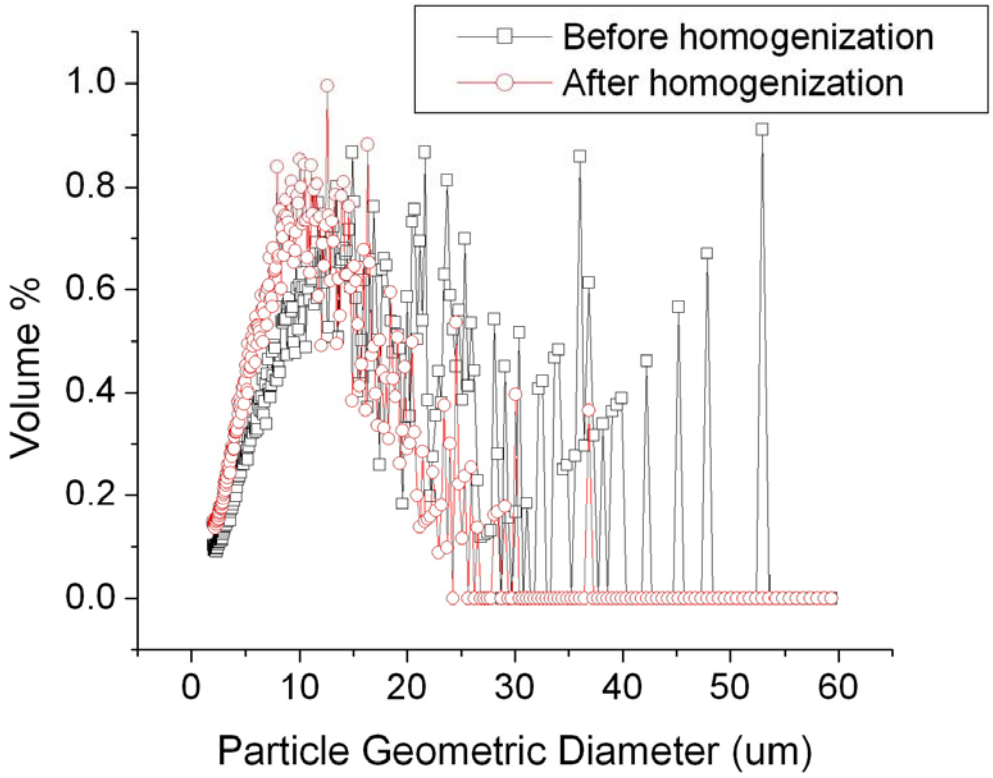

Figure A2. Percent volume as a function of particle diameter for an agglomerated solution of NIF/SA nanoparticles in water after addition of NaCl to 0.1 M. Also shown is the same solution after homogenization at 25,000 RPM for 30 seconds.

Agglomerate size may be somewhat controlled based on the amount of destabilizer that is added (Figure A3). The data reveal that a high concentration of salt leads to larger, more polydisperse agglomerations, very small amounts lead to none, while slightly larger amounts of salt can induce agglomeration and the particles remain smaller and monodisperse. This provides a controlled variable that may prove useful for future formulations.

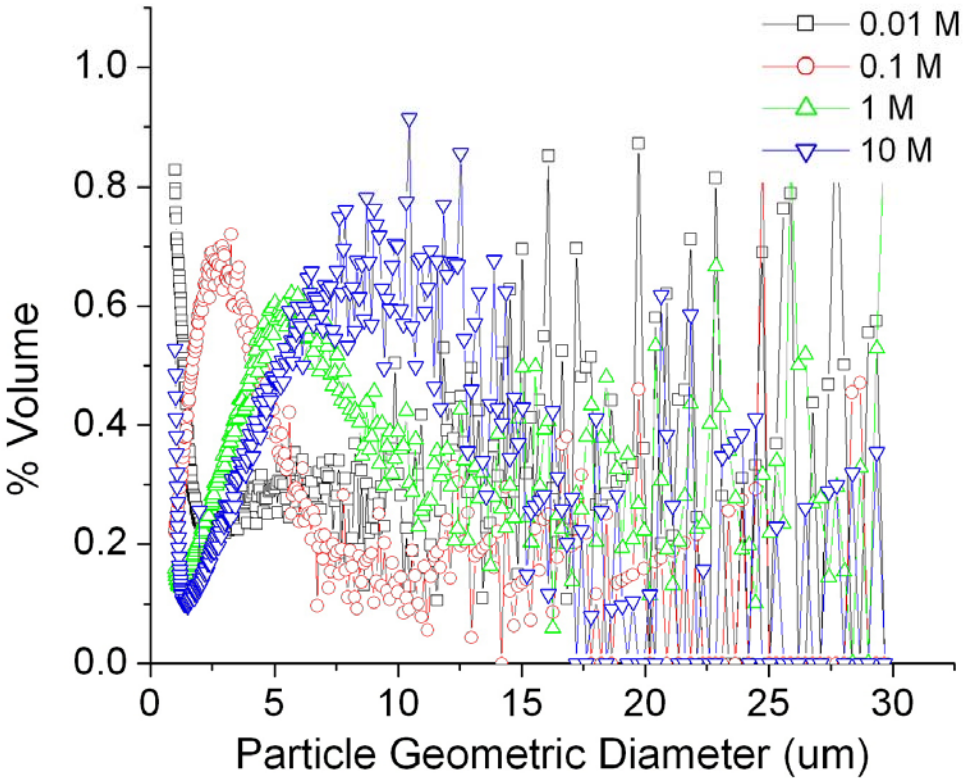

Figure A3. Particle size distributions for a sample of nanoparticle agglomerates under a range of NaCl molarities (0.01, 0.1, 1, and 10 Molar) marked from lowest to highest. Salt was added with homogenization at 15,000 RPM for 30 seconds. Figure 3.3 showed agglomerates using $MgSO_4$.

$MgSO_4$ was used as a destabilizer and the results indicated poor performance (Figure A4). The particles showed an extremely wide size distribution which was not observed with any of the other destabilizers. Also, when $MgSO_4$ was introduced into the solutions, it was noticed that a drastic temperature change occurred, and this varied with the total amount that was added (data not shown).

This was seen as another drawback with $MgSO_4$, because high temperatures can be harsh on drug entities and cause drug degradation.

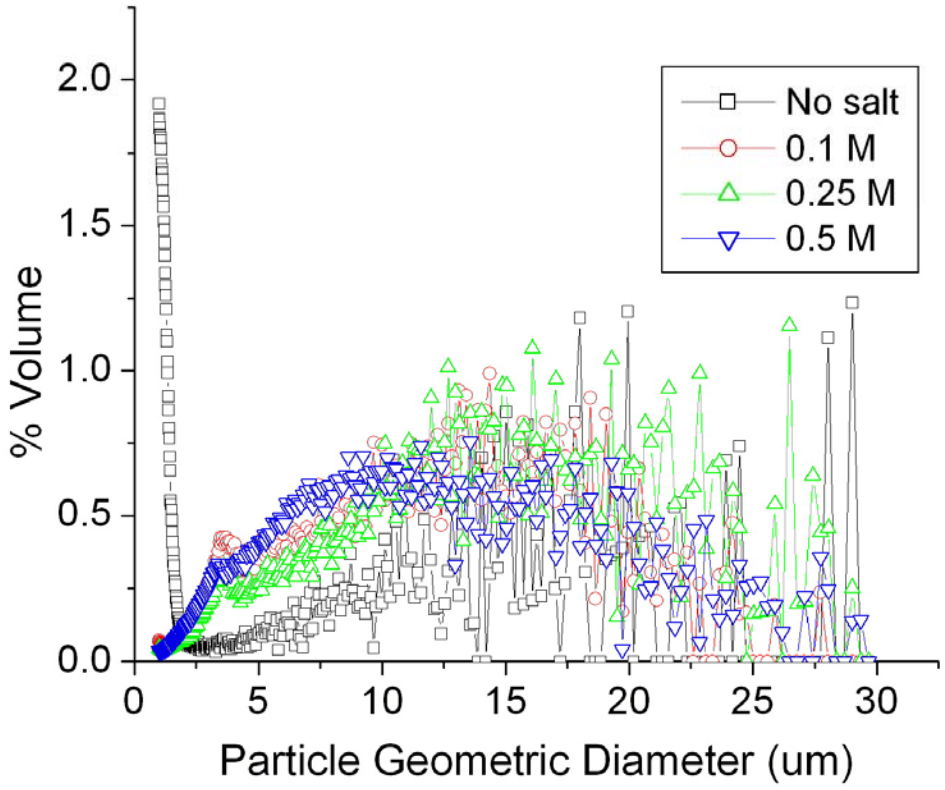

Figure A4. Particle size distributions for a nanoparticle solution and portions of the solution with MgSO4 added to vary molarities (0.1, 0.25, 0.5). Salt was added with homogenization at 15 kRPM for 30 seconds.

When used as a destabilizer, $CaCl_2$ did not reveal an exothermic reaction upon addition, and it was found to be a suitable destabilizer (Figure A5). However, the agglomerate sizes changed drastically upon application of shear force, and the final sizes were probably too small for the intended use. This may be the result of weak interactions between the divalent ions and the nanoparticles. Aside from NaCl, $CaCl_2$ was shown to be the best destabilizing salt. It would be advantageous to continue studies with both salts in the future. Special attention should be paid to minimizing salt content while maintaining proper agglomeration.

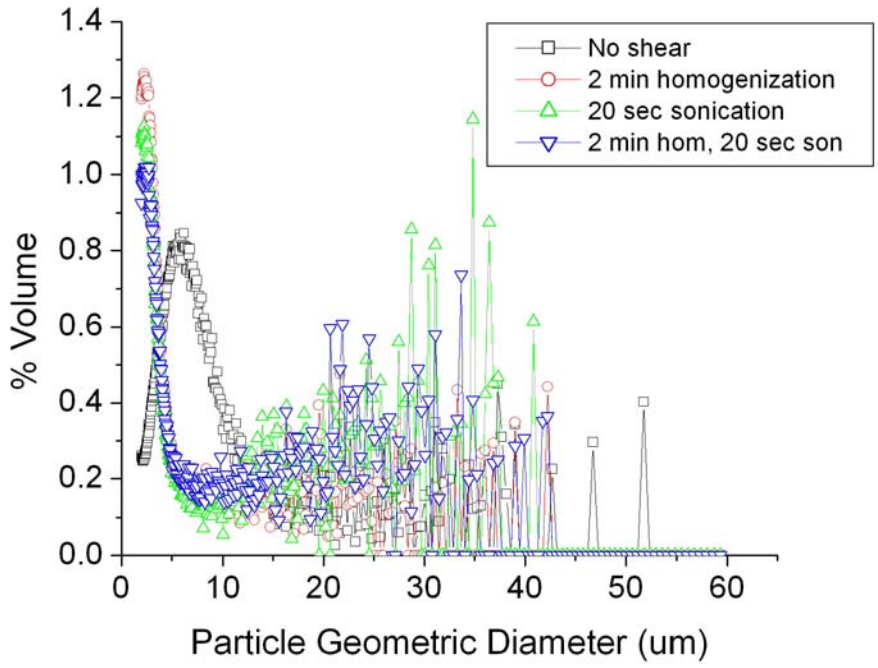

Figure A5. The effects of sonication and homogenization on a agglomerated suspension of nanoparticles. A solution of nanoparticles was allowed to agglomerate to completion under 0.1M CaCl2, and portions were subject to homogenization at 15 kRPM for 2 minutes, and sonication at 60% amplitude for 20 seconds.

B. Cascade Impactor

The cascade impactor has been used for decades to help analyze the deposition of particulates in the human pulmonary airways without performing actual in vivo experiments. The device simulates the deposition behavior in all layers of the lung. A general schematic is shown in figure A5.

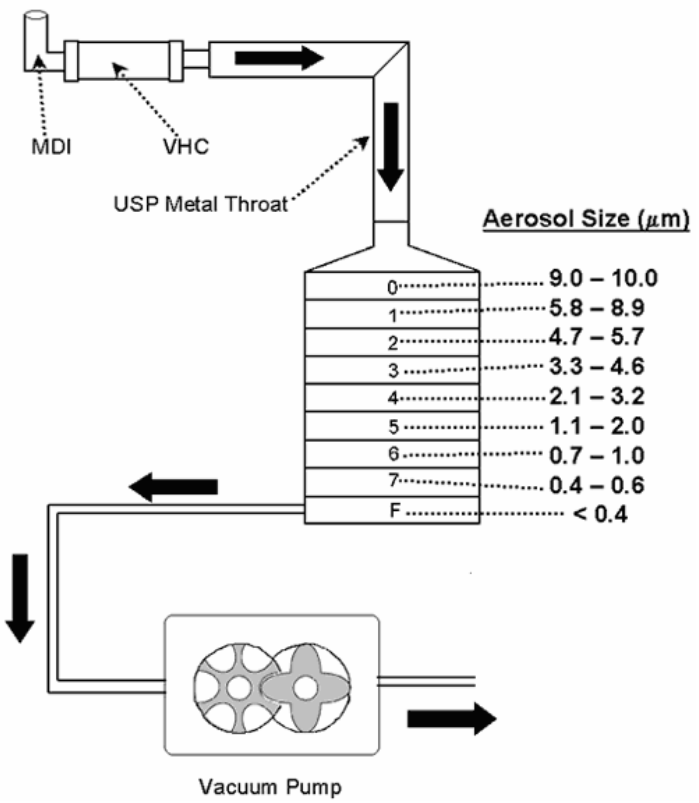

Figure A5. Schematic of a typical Anderson cascade impactor. Adapted from Reference: Pharacotherapy, copyright 2003 Pharmacotherapy Publications

Figure A5 shows the various stages of a typical cascade impactor and also diagrams how air is expected to flow through the device. A vacuum pump sucks air continually through the stack of filters and each filter catches particles

depending on their size. The cutoff size ranges based on filter number are shown again in figure A7, along with a diagram of where those sizes will typically deposit in the lung.

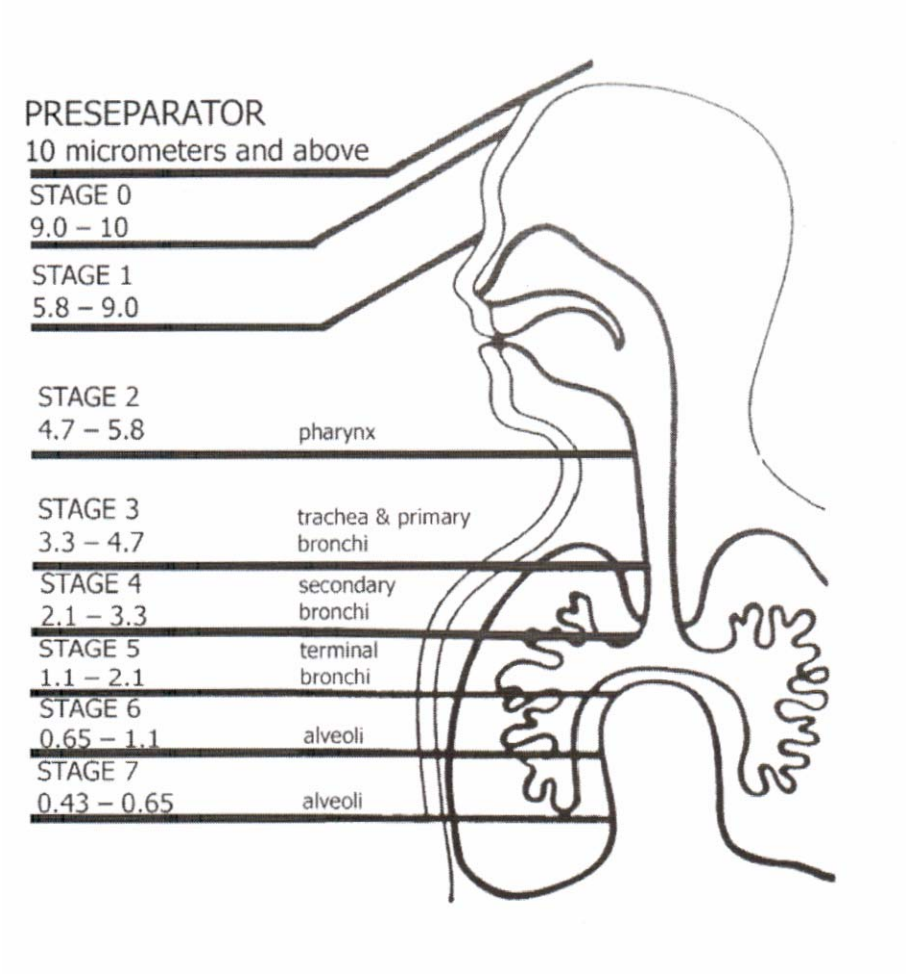

Figure A7. Schematic representation of the relationship between particle size, stage number and final deposition region in the pulmonary airways for an Anderson cascade impactor. Adapted from Reference: Operations Manual, Model 20-800 Ambient Cascade Impactor (non-viable), Tisch Environmental, Inc. June 1999.

Particle deposition in the impactor occurs via inertial impaction. Each stage has an inlet and an outlet. The inlet is composed of tiny orifices that get smaller as the stage number increases. The orifices push the air through at varying speeds. The stage holds a filter that the air must move around to reach the outlet. Some particles will not be able to stay in the air as the stream moves around the filter and they impact on the filter. Smaller particles with a lower momentum stay in the air and move on to the next filter, where they may be impacted. Higher stage numbers bear faster velocities and so smaller particles are able to gain enough momentum to impact on the stage. A diagram of the impaction event is shown in figure A6.

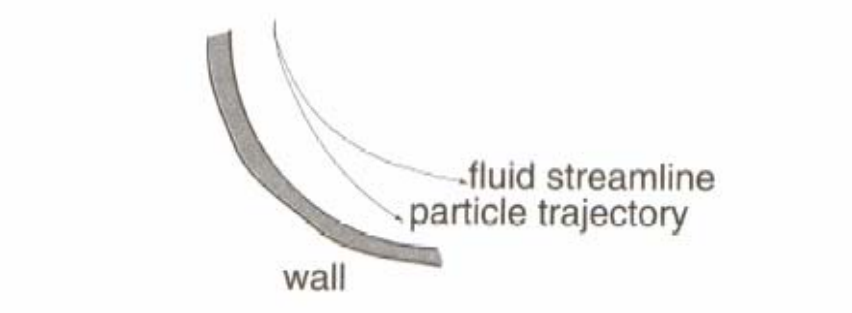

Figure A6. Diagram of impaction event such as those that occur within a cascade impactor. Adapted from Reference: Finlay, 2001. The Mechanics of Inhaled Pharmaceuticals, an introduction.

References

1. Edwards DA, Ben-Jebria A, Langer R. 1998. Recent advances in pulmonary drug delivery using large, porous inhaled particles. ed.: Am Physiological Soc. p 379-385.

2. Roco MC, Bainbridge WS 2002. Converging Technologies for Improving Human Performance: Integrating From the Nanoscale. Journal of Nanoparticle Research 4(4):281-295.

3. Müller RH, Jacobs C, Kayser O 2001. Nanosuspensions as particulate drug formulations in therapy Rationale for development and what we can expect for the future. Advanced Drug Delivery Reviews 47(1):3-19.

4. Kumar M 2000. Nano and microparticles as controlled drug delivery devices. J Pharm Pharm Sci 3(2):234–258.

5. Groneberg DA, Witt C, Wagner U, Chung KF, Fischer A 2003. Fundamentals of pulmonary drug delivery. Respiratory Medicine 97(4):382-387.

6. Edwards DA, Hanes J, Caponetti G, Hrkach J, Ben-Jebria A, Eskew ML, Mintzes J, Deaver D, Lotan N, Langer R 1997. Large Porous Particles for Pulmonary Drug Delivery. Science 276(5320):1868.

7. Pritchard JN 2001. The Influence of Lung Deposition on Clinical Response. Journal of Aerosol Medicine 14(1, Supplement 1):19-26.

8. Raimondi AC 1997. Treatment of acute severe asthma with inhaled albuterol delivered via jet nebulizer, metered dose inhaler with spacer, or dry powder. Chest 112(1):24-28.

9. Langer R 1998. Drug delivery and targeting. Nature 392(6679 Suppl):5-10.

10. Patton JS. 2004. The Promise of Pulmonary Drug Delivery. ed.: The Drug Delivery Report. p 35-38.

11. Ashurst I, Malton A, Prime D, Sumby B 2000. Latest advances in the development of dry powder inhalers. Pharmaceutical Science & Technology Today 3(7):246-256.

12. Yeh HC, Schum GM 1980. Models of human lung airways and their application to inhaled particle deposition. Bulletin of Mathematical Biology 42(3):461-480.

13. Finlay WH. 2001. The Mechanics of Inhaled Pharmaceutical Aerosols: An Introduction. ed.: Academic Press.

14. Byron PR 1986. Prediction of Drug Residence Times in Regions of the Human Respiratory Tract Following Aerosol Inhalation. Sciences 75(5).

15. Dunbar C, Scheuch G, Sommerer K, DeLong M, Verma A, Batycky R 2002. In vitro and in vivo dose delivery characteristics of large porous particles for inhalation. International Journal of Pharmaceutics 245(1-2):179-189.

16. DeCarlo P, Slowik JG, Worsnop DR, Davidovits P, Jimenez JL 2004. Particle Morphology and Density Characterization by Combined Mobility and Aerodynamic Diameter Measurements. Part 1: Theory. Aerosol Science and Technology 38(12):1185-1205.

17. Mobley C, Hochhaus G 2001. Methods used to assess pulmonary deposition and absorption of drugs. Drug Discovery Today 6(7):367-375.

18. Patton JS, Byron PR 2007. Inhaling medicines: delivering drugs to the body through the lungs. Nat Rev Drug Discov 6(1):67-74.

19. Berg E 1995. In vitro properties of pressurized metered dose inhalers with and without spacer devices. J Aerosol Med 8(3):S3-10.

20. Wetterlin K 1988. Turbuhaler: A New Powder Inhaler for Administration of Drugs to the Airways. Pharmaceutical Research 5(8):506-508.

21. Fiegel J, Garcia-Contreras L, Thomas M, VerBerkmoes J, Elbert K, Hickey A, Edwards D 2008. Preparation and in Vivo Evaluation of a Dry Powder for Inhalation of Capreomycin. Pharmaceutical Research 25(4):805-811.

22. Labiris NR, Dolovich MB 2003. Pulmonary drug delivery. Part II: The role of inhalant delivery devices and drug formulations in therapeutic effectiveness of aerosolized medications. British journal of clinical pharmacology 56(6):600-612.

23. Mazela J, Merritt T, Finer NN 2007. Aerosolized surfactants. Current Opinion in Pediatrics 19(2):155.

24. Anzueto A, Baughman RP, Guntupalli KK, Weg JG, Wiedemann HP, Raventos AA, Lemaire F, Long W, Zaccardelli DS, Pattishall EN 1996. Aerosolized Surfactant in Adults with Sepsis-Induced Acute Respiratory Distress Syndrome. New England Journal of Medicine 334(22):1417.

25. Taeusch HW, Lu K, Ramierez-Schrempp D 2002. Improving pulmonary surfactants. Acta Pharmacol Sin 4083:11-15.

26. Takeuchi H, Yamamoto H, Kawashima Y 2001. Mucoadhesive nanoparticulate systems for peptide drug delivery. Advanced Drug Delivery Reviews 47(1):39-54.

27. Louey MD, Van Oort M, Hickey AJ 2004. Aerosol Dispersion of Respirable Particles in Narrow Size Distributions Using Drug-Alone and Lactose-Blend Formulations. Pharmaceutical Research 21(7):1207-1213.

28. Gonda I 1991. Physico-chemical Principles in Aerosol Delivery. Topics in Pharmaceutical Sciences 1991:95-113.113.

29. Cook RO, Pannu RK, Kellaway IW 2005. Novel sustained release microspheres for pulmonary drug delivery. Journal of Controlled Release 104(1):79-90.

30. Lai YL, Mehta RC, Thacker AA, Yoo SD, McNamara PJ, DeLuca PP 1993. Sustained Bronchodilation with Isoproterenol Poly (Glycolide-co-Lactide) Microspheres. Pharmaceutical Research 10(1):119-125.

31. Fu J, Fiegel J, Krauland E, Hanes J 2002. New polymeric carriers for controlled drug delivery following inhalation or injection. Biomaterials 23(22):4425-4433.

32. Yamamoto H, Kuno Y, Sugimoto S, Takeuchi H, Kawashima Y 2005. Surface-modified PLGA nanosphere with chitosan improved pulmonary delivery of calcitonin by mucoadhesion and opening of the intercellular tight junctions. Journal of Controlled Release 102(2):373-381.

33. Grotberg JB 1994. Pulmonary Flow and Transport Phenomena. Annual Reviews in Fluid Mechanics 26(1):529-571.

34. Meibohm B, NetLibrary I. 2007. Pharmacokinetics and Pharmacodynamics of Biotech Drugs: Principles and Case Studies in Drug Development. ed.: Wiley-VCH.

35. Imai T, Yoshigae Y, Hosokawa M, Chiba K, Otagiri M 2003. Evidence for the involvement of a pulmonary first-pass effect via carboxylesterase in the disposition of a propranolol ester derivative after intravenous administration. Journal of Pharmacology and Experimental Therapeutics:103056499.

36. Svartengren K, Lindestad PA, Svartengren M, Bylin G, Philipson K, Camner P 1994. Deposition of inhaled particles in the mouth and throat of asthmatic subjects. European Respiratory Journal 7(8):1467.

37. Semmler-Behnke M, Takenaka S, Fertsch S, Wenk A, Seitz J, Mayer P, Oberdörster G, Kreyling WG 2007. Efficient Elimination of Inhaled Nanoparticles from the Alveolar Region: Evidence for Interstitial Uptake and Subsequent Reentrainment onto Airways Epithelium. Environmental Health Perspectives 115(5):728.

38. Piknova B, Schram V, Hall SB 2002. Pulmonary surfactant: phase behavior and function. Current Opinion in Structural Biology 12(4):487-494.

39. Gonda I 1992. Targeting by deposition. Pharmaceutical Inhalation Aerosol Technology:61–82.

40. Kitson C, Angel B, Judd D, Rothery S, Severs NJ, Dewar A, Huang L, Wadsworth SC, Cheng SH, Geddes DM The extra-and intracellular barriers to lipid and adenovirus-mediated pulmonary gene transfer in native sheep airway epithelium.

41. Hornby PJ, Abrahams TP 1996. Pulmonary Pharmacology. Clinical Obstetrics and Gynecology 39(1):17.

42. Lai SK, O'Hanlon DE, Harrold S, Man ST, Wang YY, Cone R, Hanes J 2007. Rapid transport of large polymeric nanoparticles in fresh undiluted human mucus. Proceedings of the National Academy of Sciences 104(5):1482.

43. Wiedmann TS, Bhatia R, Wattenberg LW 2000. Drug solubilization in lung surfactant. Journal of Controlled Release 65(1-2):43-47.

44. Lu Y, Chen SC 2004. Micro and nano-fabrication of biodegradable polymers for drug delivery. Advanced Drug Delivery Reviews 56(11):1621-1633.

45. Rasenack N, Steckel H, Mueller BW 2003. Micronization of anti-inflammatory drugs for pulmonary delivery by a controlled crystallization process. Journal of Pharmaceutical Sciences 92(1):35-44.

46. Landfester K 2003. Miniemulsions for nanoparticle synthesis. Top Curr Chem 227:75-123.

47. Soppimath KS, Aminabhavi TM, Kulkarni AR, Rudzinski WE 2001. Biodegradable polymeric nanoparticles as drug delivery devices. Journal of Controlled Release 70(1-2):1-20.

48. Mehnert W, Mäder K 2001. Solid lipid nanoparticles Production, characterization and applications. Advanced Drug Delivery Reviews 47(2-3):165-196.

49. Zimmermann A, Elema MR, Hansen T, Müllertz A, Hovgaard L 2007. Determination of surface-adsorbed excipients of various types on drug particles prepared

by antisolvent precipitation using HPLC with evaporative light scattering detection. Journal of Pharmaceutical and Biomedical Analysis 44(4):874-880.

50. Lince F, Marchisio D, Jawor-Baczynska A, Sefcik J, Barresi A 2007. Turbulent Precipitation of Nanoparticles through Solvent Displacement. The 2007 Annual Meeting.

51. Matteucci ME, Hotze MA, Johnston KP, Williams RO 2006. Drug nanoparticles by antisolvent precipitation: Mixing energy versus surfactant stabilization. Langmuir 22(21):8951-8959.

52. Subramaniam B, Rajewski RA, Snavely K 1997. Pharmaceutical processing with supercritical carbon dioxide. Journal of Pharmaceutical Sciences 86(8):885-890.

53. Steckel H, Thies J, Müller BW 1997. Micronizing of steroids for pulmonary delivery by supercritical carbon dioxide. International Journal of Pharmaceutics 152(1):99-110.

54. Kerc J, Srcic S, Knez Ž, Sencar-Božic P 1999. Micronization of drugs using supercritical carbon dioxide. International Journal of Pharmaceutics 182(1):33-39.

55. He P, Davis SS, Illum L 1999. Chitosan microspheres prepared by spray drying. International Journal of Pharmaceutics 187(1):53-65.

56. Chawla A, Taylor KMG, Newton JM, Johnson MCR 1994. Production of spray dried salbutamol sulphate for use in dry powder aerosol formulation. International Journal of Pharmaceutics 108(3):233-240.

57. Huang YC, Yeh MK, Cheng SN, Chiang CH 2003. The characteristics of betamethasone-loaded chitosan microparticles by spray-drying method. Journal of Microencapsulation 20(4):459-472.

58. Sham JOH, Zhang Y, Finlay WH, Roa WH, Löbenberg R 2004. Formulation and characterization of spray-dried powders containing nanoparticles for aerosol delivery to the lung. International Journal of Pharmaceutics 269(2):457-467.

59. Videira MA, Botelho MF, Santos AC, Gouveia LF, de Lima JJP, Almeida AJ 2002. Lymphatic Uptake of Pulmonary Delivered Radiolabelled Solid Lipid Nanoparticles. Journal of Drug Targeting 10(8):607-613.

60. Zhang Q, Shen Z, Nagai T 2001. Prolonged hypoglycemic effect of insulin-loaded polybutylcyanoacrylate nanoparticles after pulmonary administration to normal rats. International Journal of Pharmaceutics 218(1-2):75-80.

61. Shi L, Plumley CJ, Berkland C 2007. Biodegradable Nanoparticle Flocculates for Dry Powder Aerosol Formulation. Langmuir 23(22):10897-10901.

62. Malcolmson RJ, Embleton JK 1998. Dry powder formulations for pulmonary delivery. Pharmaceutical Science & Technology Today 1(9):394-398.

63. Steckel H, Brandes HG 2004. A novel spray-drying technique to produce low density particles for pulmonary delivery. International Journal of Pharmaceutics 278(1):187-195.

64. Swarbrick J, Boylan JC. 2000. Encyclopedia of Pharmaceutical Technology. ed.: Dekker.

65. Time M 1970. Changes in Morphology with Milling of the Commercial Microcrystalline Cellulose. JOURNAL OF APPLIED POLYMER SCIENCE 14.

66. Sacchetti M, Van Oort MM 1996. Spray-drying and supercritical fluid particle generation techniques. Inhalation Aerosols: Physical and Biological Basis for Therapy Marcel Dekker, New York:337–384.

67. Jain RA 2000. The manufacturing techniques of various drug loaded biodegradable poly (lactide-co-glycolide)(PLGA) devices. Biomaterials 21(23):2475-2490.

68. Ganderton D, Kassem NM 1992. Dry powder inhalers. Advances in Pharmaceutical Sciences 6:165–191.

69. Karhu M, Kuikka J, Kauppinen T, Bergström K, Vidgren M 2000. Pulmonary deposition of lactose carriers used in inhalation powders. International Journal of Pharmaceutics 196(1):95-103.

70. French DL, Edwards DA, Niven RW 1996. The influence of formulation on emission, deaggregation and deposition of dry powders for inhalation. Journal of Aerosol Science 27(5):769-783.

71. Zeng XM, Martin GP, Marriott C, Pritchard J 2001. Lactose as a carrier in dry powder formulations: The influence of surface characteristics on drug delivery. Journal of Pharmaceutical Sciences 90(9):1424-1434.

72. Steckel H, Müller BW 1998. Metered-dose inhaler formulation of fluticasone-17-propionate micronized with supercritical carbon dioxide using the alternative propellant HFA-227. International Journal of Pharmaceutics 173(1-2):25-33.

73. Kwon JH, Lee BH, Lee JJ, Kim CW 2004. Insulin microcrystal suspension as a long-acting formulation for pulmonary delivery. European Journal of Pharmaceutical Sciences 22(2-3):107-116.

74. Zhang QY, Kaminsky LS, Dunbar D, Zhang J, Ding X 2007. Role of Small Intestinal Cytochromes P450 in the Bioavailability of Oral Nifedipine. Drug Metabolism and Disposition 35(9):1617-1623.

75. Wachter RM 1987. Symptomatic hypotension induced by nifedipine in the acute treatment of severe hypertension. Archives of Internal Medicine 147(3):556-558.

76. Ricciardi MJ, Bossone E, Bach DS, Armstrong WF, Rubenfire M. 1999. Echocardiographic Predictors of an Adverse Response to a Nifedipine Trial in Primary Pulmonary Hypertension* Diminished Left Ventricular Size and Leftward Ventricular Septal Bowing. ed.: Am Coll Chest Phys. p 1218-1223.

77. Furberg CD, Psaty BM, Meyer JV 1995. Nifedipine Dose-Related Increase in Mortality in Patients With Coronary Heart Disease. Circulation 92(5):1326-1331.

78. Friedrich H, Nada A, Bodmeier R 2005. Solid State and Dissolution Rate Characterization of Co-Ground Mixtures of Nifedipine and Hydrophilic Carriers. Drug Development and Industrial Pharmacy 31(8):719-728.

79. Kloner RA 1995. Nifedipine in Ischemic Heart Disease. Circulation 92(5):1074-1078.

80. Hedner T 1986. Calcium channel blockers: spectrum of side effects and drug interactions. Acta Pharmacol Toxicol (Copenh) 58(2):119-130.

81. Lavy A 1999. Corrosive Effect of Nifedipine in the Upper Gastrointestinal Tract. Diagnostic and Therapeutic Endoscopy 6(1):39-41.

82. Sencar-Božic P, Srcic S, Knez Z, Kerc J 1997. Improvement of nifedipine dissolution characteristics using supercritical CO2. International Journal of Pharmaceutics 148(2):123-130.

83. Kamiya S, Yamada M, Kurita T, Miyagishima A, Arakawa M, Sonobe T 2007. Preparation and stabilization of nifedipine lipid nanoparticles. International Journal of Pharmaceutics.

84. Grundy JS, Kherani R, Foster RT 1912. Photostability determination of commercially available nifedipine oral dosage formulations. J Pharm Biomed Anal 1994:1529-1535.

85. Aulton ME. 1988. Pharmaceutics: the science of dosage form design. ed.: Churchill Livingstone, Edinburgh; New York.

86. Kumar V, Kothari SH, Banker GS 2001. Compression, compaction, and disintegration properties of low crystallinity celluloses produced using different agitation rates during their regeneration from phosphoric acid solutions. AAPS PharmSciTech 2(2):7.

87. Mendez-Alcaraz JM, D'Aguanno B, Klein R 1992. Structure of binary colloidal mixtures of charged and uncharged spherical particles. Langmuir 8(12):2913-2920.

88. Rosa D, Catalá A 1998. Fatty Acid Profiles and Non Enzymatic Lipid Peroxidation of Microsomes and Mitochondria from Bovine Liver, Kidney, Lung and Heart. Archives Of Physiology And Biochemistry 106(1):33-37.

89. Ilett KF, Stripp B, Menard RH, Reid WD, Gillette JR 1974. Studies on the mechanism of the lung toxicity of paraquat: Comparison of tissue distribution and some biochemical parameters in rats and rabbits. Toxicology and Applied Pharmacology 28(2):216-226.

90. Parkville V 1990. Peter R. Hutchison1 and Thomas W. Healy2 Chemicals Division Tioxide Australia Pty. Ltd. Burnie, Tasmania Department of Physical Chemistry. Surface and Colloid Chemistry in Natural Waters and Water Treatment.

91. Kawabe Y, Nakamura H, Hino E, Suzuki S 2008. Photochemical stabilities of some dihydropyridine calcium-channel blockers in powdered pharmaceutical tablets. Journal of Pharmaceutical and Biomedical Analysis.

92. el Walily AF 1997. Simultaneous determination of the binary mixture of nifedipine and mefruside using derivate spectroscopy, capillary gas-liquid chromatography and high performance liquid chromatography. Acta Pharm Hung 67(2-3):89-97.

93. Katz SL, Adatia I, Louca E, Leung K, Humpl T, Reyes JT, Coates AL 2006. Nebulized therapies for childhood pulmonary hypertension: An in vitro model. Pediatr Pulmonol 41(7):666-673.